GLACIER CONTRIBUTION TO LOWLAND STREAMFLOW: A MULTI-YEAR, GEOCHEMICAL HYDROGRAPH SEPARATION STUDY IN SUB-ARCTIC ALASKA

By

Tiffany A. Gatesman, B.S.

A Thesis Submitted in Partial Fulfillment of the Requirements
for the Degree of

MASTER OF SCIENCE
in
Environmental Chemistry

University of Alaska Fairbanks

December 2017

Approved:

Thomas P. Trainor, Co-Chair
Anna K. Liljedahl, Co-Chair
Thomas A. Douglas, Committee Member
Thomas K. Green, *Department of Chemistry and Biochemistry Chair*
Paul Layer, Dean
College of Natural Science and Mathematics
Michael Castellini, *Dean of the Graduate School*

Abstract

Glacier melt affects the geochemical composition of rivers; however, quantifying the glacier contribution to subarctic watershed-scale runoff has attracted limited attention. To estimate glacier contribution, we conducted a 6-year geochemical hydrograph separation study in a geologically heterogeneous glacierized watershed in Interior Alaska. Water samples were collected daily from Jarvis Creek during late April through September. Source waters were collected synoptically each year from rain, snow, baseflow (winter discharge), and the glacier terminus discharge. All samples were analyzed for stable water isotopes and dissolved ion concentrations. Stream surface water samples have large seasonal and inter-annual geochemical variation, however, source waters show distinct chemical signatures allowing the application of a geochemical hydrograph separation model to quantify relative source contribution to lowland streamflow. Considerable inter-annual differences within source water signatures emphasize the importance in informing the model with source waters sampled for each season. We estimated a seasonal average of 35% (20 to 44%) glacier terminus discharge contribution with a daily range of 2 (May) to 80% (September). If glacier contribution was to cease completely, stream discharge would be reduced by 48% and 22% in low and high rainfall summers, respectively. Combined with the documented shrinkage of glaciers, our findings emphasizes the need for further research on glacial wastage effect on subarctic watersheds.

Table of Contents

List of Figures

Page

List of Tables

Page

Chapter 1

Appendices

List of Appendices

Page

Introduction

1. Introduction

Climate determines the mass balance of glaciers (Gillespie and Molnar, 1995; Lemke et al., 2007). Therefore, any change in climate may result in major alterations in the release of stored water from glaciers (Cogley et al., 2011). This is important for watershed hydrology as glaciers can supply a significant amount of water during seasonally warm and dry periods (Hannah et al., 2005; Radić and Hock, 2010; La Frenierre and Mark, 2014). Contribution from glacier melt to overall watershed-scale discharge is rarely assessed in glacier mass projections (Radić and Hock, 2010), which results in significant uncertainty in regards to altered runoff regimes and water supply to communities and agriculture activities.

Glacier covered watersheds supply water that can be used by local communities for a variety of purposes including agriculture, energy, and fisheries activities. As a consequence, the climate warming and loss of water storage could directly affect local communities as some of the most dramatic glacial advances and retreats are occurring within populated glacierized watersheds (Gillespie and Molnar, 1995). Berthier and others (2010) surveyed a 67% area of the Alaska Range over 51 years and measured an ice loss 4.33 +/- 1.4 km^3yr^{-1} water equivalent, and area average mass balance of -0.30 +/-0.09 $mmyr^{-1}$ water equivalent. The Tanana River watershed that drains primarily the north side of the Alaska Range has a decreased glacier coverage of 12% during 1950-2010 (Liljedahl et al., 2017). More specifically, Jarvis Glacier and Gulkana Glacier which drain the north slope of the Alaska Range have an average mass balance of -1,900 mm (2015-2016) and -520 mm (1966-2016), respectively (Liljedahl et al., 2017). Liljedahl and others (2017) also determined a bare ice retreat of ~1,600 meters (1949-2015) of Jarvis Glacier and reported a 2,000 meter retreat of Gulkana Glacier (1966-2015). The significance of ice loss and negative mass balances for Alaska necessitates understanding of quantifying glacial contribution to watershed hydrology.

There are multiple approaches for quantifying glacial melt contribution to stream flow. Methodological approaches include direct discharge measurement, hydrological balance equations, hydrological modeling, and the use of geochemical tracers (La Frenierre and Mark, 2014). Geochemical hydrograph separation is produced by a mixing model, which is constrained by unique chemical end-member signatures (Genereaux and Hooper, 1998; Suecker et al., 2000;

Bhatia et al., 2011; Cable et al., 2011; Klaus and McConnel, 2013; La Frenierre and Mark, 2014; Arendt et al., 2015). Using geochemical tracers as a proxy for quantifying glacier melt requires limited chemical sampling suites and does not require complex physical hydrological parameters (La Frenierre and Mark, 2014). As a consequence, this method is well suited for understanding resource management related to climate change in watersheds with limited data, limited accessibility and that are un-gauged (Baraer et al., 2009; Kong and Pong, 2012).

Geochemical hydrograph separation can also quantify and differentiate source contribution to streamflow by using multiple equations to describe water balance (La Frenierre and Mark, 2013). In theory, solute composition can be used to infer the contribution of unique reservoirs via a chemical mixing model. Electrical conductivity and dissolved solutes can be used as end-member tracers, but they have non-conservative behavior and are subject to alterations and enrichment during mixing (Bhatia et al., 2011). Stable water isotopes are widely used in mixing models since their chemical properties differ (Bhatia et al., 2011). Geochemical modeling solely using stable water isotopes began in the 1960's with a simple 2-component model differentiating pre-event and event waters (Klaus and McDonnell, 2013). With recent advances in research over the past 20 years, this simple 2-component method is being extended to more complex models (Klaus and McConnel, 2013).

2. Stable water isotopes

Stable water isotopes are often used in chemical hydrograph separation models. These isotopes are recorded as the ratio of heavy over light isotopes and are recorded in per mil (‰) which is the deviation from the standard water sample of the ocean near the equator (Vienna Standard Mean Ocean Water (VSMOW); Mook, 2000) and symbolized with a delta (δ) sign,

$$\delta^{18}O \text{ or } \delta D = \left(\frac{R_{sample}}{R_{standard}} - 1\right) * 1000 \qquad (3)$$

where R_{sample} is the isotopic ratio of heavy or light ($D/^{1}H$ or $^{18}O/^{16}O$) and $R_{standard}$ is VSMOW (Klaus and McDonnell, 2013). Stable water isotope $\delta^{18}O$ and δD variation is dependent on temperature and the hydrologic cycle and, therefore have unique signatures for different reservoirs (Buttle, 1998; Kendall and Caldwell, 1998; Frenierre and Mark, 2013; Klaus and McDonnell, 2013). Meteoric waters develop unique isotopic signatures due to kinetic fractionation and thermodynamics. Bonds between lighter isotopes can be broken more easily during phase changes

than heavy isotopes resulting in an enrichment of heavy isotopes in the reactants (Ingraham, 1998; Kendall and Caldwell, 1998). This process, in turn, causes condensed precipitation to become isotopically lighter in high latitude and high elevation airsheds (Cooper, 1998; Ingraham, 1998; Faure and Mensing, 2005), such as the ones over Interior Alaska.

Isotopic content in water vapor is dependent on environmental factors such as temperature during condensation and evaporation, type of storm systems, and trajectory of the air mass. Storm systems affect the isotopic content of precipitation depending on where the air mass originated (i.e. ocean, lake, evapotranspiration, etc.) and type of storm (i.e. frontal, orographic, convective, fog, etc.) (Ingraham, 1998). In addition, smaller rainstorms are generally more enriched in heavy isotopes than larger storms. This may be a result of fractionation from parent air mass evolution or precipitation passing through relatively low humidity (Ingraham, 1998).

In glacier covered watersheds, snow carries enriched signatures of recent precipitation while glacial ice has more depleted signatures from prior deposition at higher elevations (Bhatia et al., 2011). Unique stable water isotope end-member signatures are effectively used to differentiate precipitation, glacier ice and snow, while dissolved ions are most effective for differentiating groundwater and baseflow from other sources such as glacier runoff (Mark and Seltzer, 2003; Baraer et al., 2009; Kong and Pong, 2012; La Frenierre and Mark, 2014)

The covariance between $\delta^{18}O$ and δD of precipitation can be explained by the condensation of water vapor when conditions are near equilibrium (Ingraham, 1998). The plotted relationship between $\delta^{18}O$ and δD is referred to as the Meteoric Water Line (MWL) and can be used to explain the global MWL (GMWL; Figure 1) or local (LMWL) precipitation trends (Craig, 1961; Dansgaard, 1964; Coplen et al., 2015). The slope of the GMWL is defined by the International Atomic Energy Agency (IAEA) as:

$$\delta D_{VSMOW} = 8\,\delta^{18}O_{VSMOW} + 10‰ \qquad (4)$$

where *VSMOW* is the Vienna Standard Mean Ocean Water (Kendall and Caldwell, 1998; Mook, 2000). The slope varies due to kinetic fractionation during the evaporation process. When a system is at equilibrium, the vapor isotopic content equals the precipitation isotopic content, which in turn results in a slope greater than eight (Ingraham, 1998). A slope of less than eight indicate that liquid and vapor are not at isotopic equilibrium and that evaporation occurred during unsaturated relative humidity, i.e. a relative humidity less than 100%, (Kendall and Caldwell, 1998). Small water reservoirs (i.e. evapotranspiration, fog, rivers, lakes, etc.) typically have isotopic ratios relatively

enriched in heavy isotopes compared to large water bodies (i.e. ocean) because small water bodies are more likely to be affected by equilibrium fractionation in the evaporation process, which results in MWL slopes of four to seven (Ingraham, 1998). The *y*-intercept of small water bodies is not at the origin and suggests there is a lack of evaporative equilibrium due to kinetic enrichment of deuterium (Ingraham, 1998; Kendall and Caldwell, 1998). The y-intercept can be referred to as the D-excess or D-parameter, which is related to the kinetics of evaporation and condensation (Ingraham, 1998). Stable water isotope values of condensation are related to the temperature and humidity of the cloud base where the rain-out occurs (Kendall and Caldwell, 1998). Water samples enriched in heavy isotopes (samples on the upper-right section of the MWL, Figure 1) are indicative of warmer air temperatures and precipitation (rainfall); samples depleted in heavy isotopes (lower-left section of the MWL, Figure 1) are indicative of colder temperatures and precipitation (snow) (Craig, 1961). Per this relationship, stable water isotopes can be used as hydrologic chemical tracers in hydrograph separation.

3. Glacier hydrology and geochemistry

Glaciers have multiple drainage systems that contribute unique suspended loads to streamflow (Kido et al., 2007). Geochemical weathering during post-mixing of waters affects chemical composition of streamflow (Brown et al., 1996; Richey, 1983; Tranter et al., 2011). Post-mixing chemical weathering is weathering of suspended sediment that has high reactive surface area from glacial comminution and high water-rock ratios (Brown et al., 1996). Subglacial drainage systems are complex and cannot be described solely on bulk glacier discharge (Brown et al., 1996; Tranter et al., 2002; Kido et al., 2007). The glacier drainage system during ablation season is not static due to the channel system expanding headward by control of the retreating snowline (Tranter et al., 2002). The system is separated into two main drainage compositions, distributed and discrete channels, or delayed and quick flow respectively (Raymond et al., 1995; Brown et al., 1996, Tranter et al., 2002; Kido et al., 2007). The quick flow channels are primarily basal melting, water saturated till, and glacial water storage from snow and ice melt that has been transported from water filled cavities such as crevasses and moulins (Raymond et al., 1995; Tranter et al., 2002; Kido et al., 2007). The multiple pathways contributes a varying degree of chemical characteristics. The quick flow system feeds into the delayed flow system that is characterized by a series of channels at the bed with uniform discharge and increased rock-water interactions where

chemical weathering occurs (Raymond et al., 1995; Brown et al., 1996, Tranter et al., 2002; Kido et al., 2007).

Most Earth weathering environments are driven by H_2CO_3 where CO_2 is derived from atmosphere or soil biological activity. When sulfides are present in subglacial bedrock, weathering is driven by sulfide oxidation and Fe (III) reduction by aqueous O_2. Therefore, O_2 is dominating the chemical weathering underneath glaciers rather than CO_2 (Tranter et al., 2002). The oxidation could also be enhanced by microbial activity at the base of the glacier where conditions are suboxic (Tranter et al., 2002). Sulfide oxidation coupled with carbonate and silicate dissolution are typically the dominating chemical weathering reactions in subglacial environments since carbonation is limited by the amount of CO_2 in the system (Tranter et al., 2002).

It has been previously thought that the majority of chemical weathering of glacier discharge occurs in near surface sediment layers. Brown et al., (1996) suggested that a significant proportion of dissolved solute content in glacial stream flow is due to post-mixing chemical weathering. Carbonate and sulfide reactions are also dependent on water-rock ratios, therefore, dilute waters will be dominated by carbonation reaction due to limited proton supply from sulfide oxidation (Brown et al., 1996).

A study looking at the effects of water-rock ratios, sediment crushing, repeated wetting and particle size of glacial sediment on post-mixing solute compositions was conducted in 1996 by Brown and others. They found that sulfide oxidation yielding sulfate is primarily occurring at the glacier bed and not during post-mixing. This suggests that most of the sulfide minerals remain in subglacial bedrock environment and the majority of sulfide oxidation yielding sulfate is primarily from bulk glacial melt and not from post-mixing dissolution of rock flour (Brown et al., 1996). Therefore, sulfate can be used in hydrograph separation for glacial watersheds where pyrite is present.

4. Hydrograph separation

Hydrograph separation can be used in a variety of landscapes including glacierized watersheds (Mark et al., 2005; Cable et al., 2011; Ohlanders et al., 2013; Arendt et al., 2015), land terminating outlet glaciers (Bhatia et al., 2011), watersheds influenced by only rain and snow (Taylor et al., 2002) as well as soil plots (Arendt et al., 2015). The purpose of hydrograph separation is to determine relative contributions of source inputs (for example rain and snow) into

a bulk reservoir (streamflow, aquifer etc.) by using end-members with unique chemical and isotopic signatures. There are many assumptions that ultimately leads to limitations in the model. The use of multiple components can allow the model to become less variable, and allow for more end-members and variability for large, diverse watersheds. Among the assumptions of the mixing models are that the isotopic content of the event and pre-event water are significantly different, however, this may not always be accurate. Water sources in systems are subject to a unique amount of water-rock interactions thus influencing the dissolved content of the waters. Dissolved end-member species (ions, metals, etc.) can be coupled with stable water isotopes in multi-component mixing models to differentiate waters of similar isotopic content.

Geochemical hydrograph separation can quantify and differentiate source reservoir contribution by using multiple equations to describe water balance in geologically heterogeneous alpine and glacial catchments (La Frenierre and Mark, 2014). These models can be simple or complex in regards to sample suites and mathematical techniques. Examples include simple two- and multi-component mixing models (McNamara et al., 1997; Taylor et al., 2002; Mark and Seltzer, 2003; Dahlke et al., 2013; Pu et al., 2013) and Bayesian statistical algorithm techniques (Mark et al., 2005; Bhatia et al., 2011; Cable et al., 2011; Ohlanders et al., 2013; Arendt et al., 2015). These models are often constrained with stable water isotopes but can be supported with dissolved ion species (Mark et al., 2005), radioactive radon (Bhatia et al., 2011) and silica (Klaus and McDonnell, 2013).

Two- and multi-component mixing models are used to quantify the fractional contribution of end-members to the total stream flow. The model is based on mass conservation:

$$\begin{cases} f_1 + f_2 \dots \dots + f_n = 1 \\ C_1^1 f_1 + C_2^1 f_2 \dots \dots + C_n^1 f_n = S^1 \\ \vdots \\ \vdots \\ C_1^{n-1} f_1 + C_2^{n-1} f_2 \dots \dots + C_n^{n-1} f_n = S^{n-1} \end{cases} \quad (5)$$

where f_i is a fractional contribution of the i-th end-member and $i \in (1,2,\dots,n)$, C_i^j and Q^j are concentrations of the i-th end-member and stream for the j-th tracer $j \in (1,2\dots,n-1)$ respectively (Bhatia et al., 2011). There are several assumptions in equation 5 when describing source concentrations as a distinct chemical signature (Klaus and McDonnell, 2013). The major

assumptions in stable isotope models often include (adapted from Buttle, 1998; Cable et al., 2011; Klaus and McDonnell, 2013; La Frenierre and Mark, 2014; Pu et al., 2013):

1) End-member signatures of source waters are unique
2) End-member signatures are conserved temporally and spatially throughout watershed and are not subject to any post-mixing chemical processes
3) Contributions from the soil vadose zone are minimal.

A sensitivity analysis can be used to find uncertainty on the multi-component mixing model fraction results by employing a range in end-member values associated with fractionation processes of data sampled or from literature (Bhatia et al., 2011). For example, a range of snow signatures can be used to symbolize the stable water isotopic enrichment occurring during snow melt and metamorphism of the original snow (Taylor et al., 2001; Bhatia et al., 2011). Oftentimes glacier and snow meltwater isotope values are similar (Bhatia et al., 2011), which complicates the hydrograph separation analysis unless major ion values are implemented. Statistical hydrograph separation algorithms are based on a multivariate normal distribution of data. These models incorporate the Bayesian framework, which defines the likelihood of the observed data, includes mixing models for fractional contribution of different water sources and defines prior distributions for model parameters and variance terms (Berliner et al., 1996; Ogle et al., 2004 Cable et al., 2011; Arendt et al., 2015). Uncertainties are accounted for by coupling $\delta^{18}O$ and δD observed data, directly incorporating time of year and prior assumptions (Cable et al., 2011; Arendt et al., 2015).

5. Significance of research

Glacial mass wastage is relevant for the hydrology of many rivers in Alaska because glaciers provide water and are documented to have lost mass in recent decades (Gillespie and Molnar, 1995; Hannah et al., 2005; Radić and Hock, 2010; La Frenierre and Mark, 2014). The study watershed of Jarvis Creek, Interior Alaska (Figure 2), supplies water to the Delta Junction community, its agricultural district, communities and industries within the Tanana River and Yukon River basins. Climate change will have major implications on socio-economics, specifically (1) agricultural and military land use, (2) energy development, (3) transportation planning and design, and (4) glacial melt forecasting, as further explained below:

1) The Salcha-Delta Soil and Water Conservation District (SWCD) have been involved with various hydrologic studies in Interior Alaska since 1960 when residents expressed concerns about soil and water resources related to agriculture and military activities. Climate change issues in the Delta Junction area include agriculture groundwater supply and flooding of military and private lands.
2) Engineers designing hydropower infrastructure traditionally used historical streamflow data (e.g. ~50 years) to plan for the future hydrologic conditions. These assumptions do not take into account the effects of changes in glacier wastage (March 2009 http://www.akenergyauthority.org/ SusitnaReports.html).
3) Typical bridge or dam construction is intended to operate for approximately 100 years. In that time, there may be dramatic hydrologic change exhibited by significant climate warming (IPCC 2007). The Alaska Department of Transportation and Public Facilities (AK DOTandPF) have expressed concerns regarding the limited road network of Alaska intersecting the glacial-fed rivers that may have changes in flow regimes.
4) The National Oceanic and Atmospheric Administration (NOAA) Alaskan River Forecast Center (ARFC) is also interested in understanding and representing glacier meltwater contributions in lumped-parameter forecast models. Understanding seasonal glacial meltwater routing and storage will promote more accurate flood forecasting.

Hydrograph partitioning of subarctic watershed can assist in future planning for managers and planners of streamflow change under climate warming. The effort may also further the knowledge of stable water isotope end-member mixing models for Alaskan rivers. Quantified glacial meltwater contribution using geochemical hydrograph partitioning can also be used in conjunction with stream runoff measurements to refine hydrological models.

6. Research objectives

The research presented includes a 6-year study of stable water isotopic hydrograph separation techniques coupled with dissolved ion concentrations and stream discharge measurements (Chapter 2). Hydrograph separation techniques allow the a) quantification of intra- and inter-annual variation of glacier melt contribution to lowland streamflow and b) an estimate of future runoff regimes if glacier melt vanishes. In addition, data describing watershed-scale weathering processes are included in the appendices and includes a) characterization of glacial

stream bed sediment using x-ray diffraction techniques (Appendix A) and b) colloid characterization of glacial terminus and bulk stream flow using field flow fractionation techniques (Appendix B).

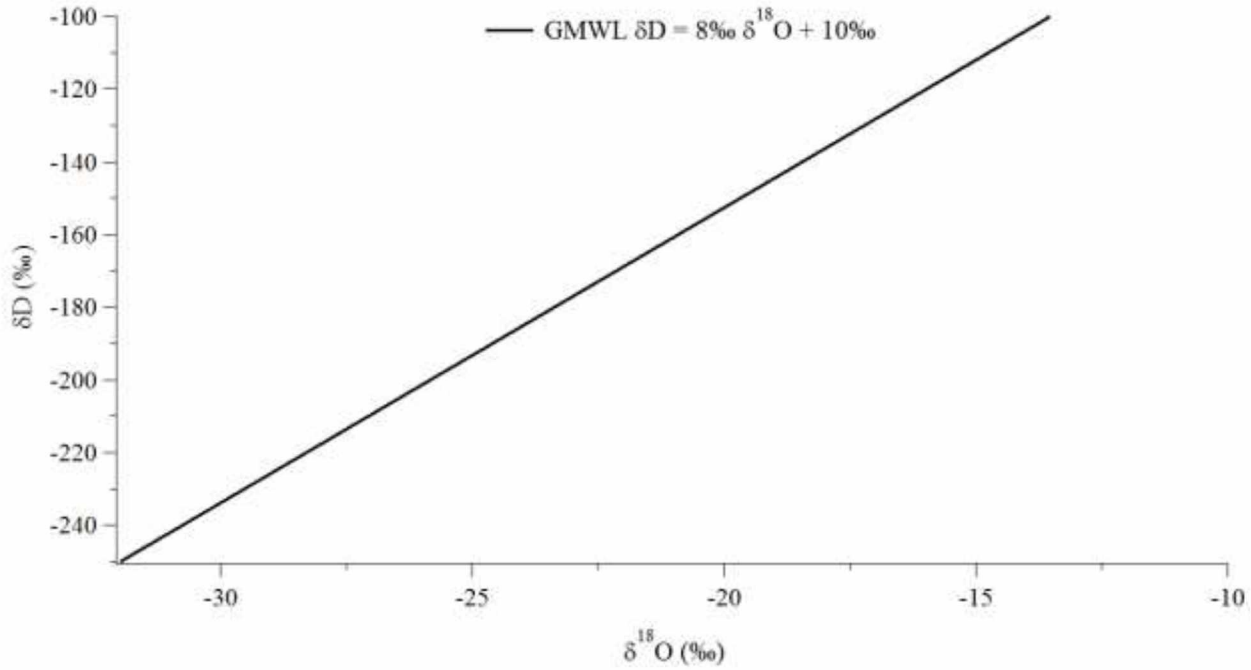

Figure 1 *Global Meteoric Water line. Covariance relationship of δD and $\delta^{18}O$ of global precipitation (δD = 8‰ $\delta^{18}O$ + 10‰). Modified from Mook (2000).*

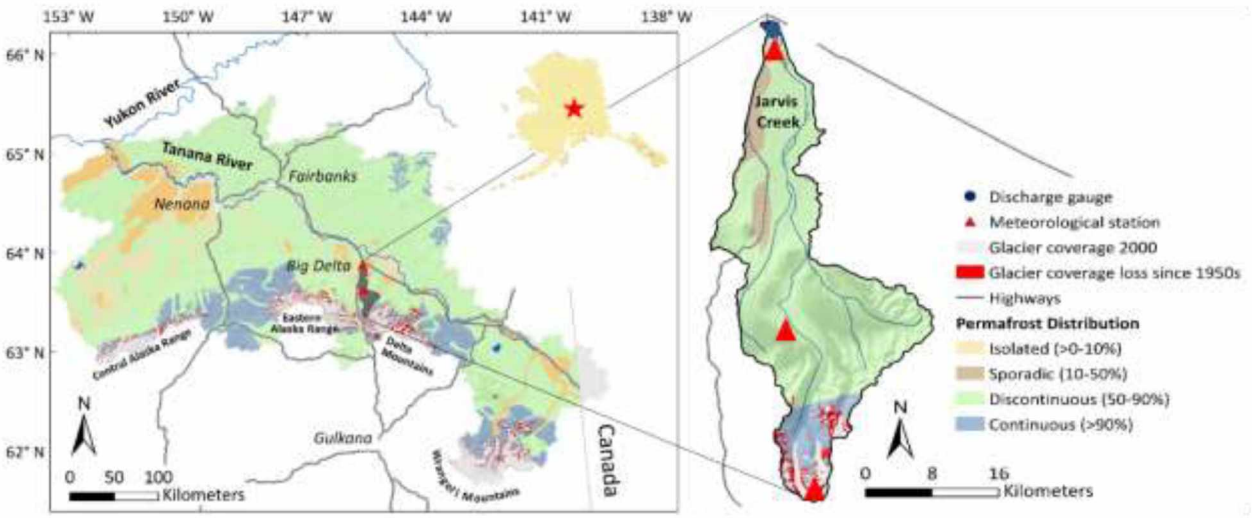

Figure 2 *Jarvis Creek Watershed. Sub-basin of the Tanana and Yukon Rivers. Watershed is 636 km^2 and is 3.3% glacierized. It has typical subarctic land features such as discontinuous permafrost, till, tundra, taiga and permanent snowfields (Jorgenson et al., 2008).*

REFERENCES

Arendt, C. A., Aciego, S. M., and Hetland, E. A. (2015). An open source Bayesian Monte Carlo isotope mixing model with applications in Earth surface processes. Geochemistry, Geophysics, Geosystems, 16(5), 1274-1292.

Baraer, M., McKenzie, J. M., Mark, B. G., Bury, J., & Knox, S. (2009). Characterizing contributions of glacier melt and groundwater during the dry season in a poorly gauged catchment of the Cordillera Blanca (Peru). Advances in Geosciences, 22, 41-49.

Berliner, L. M. (1996). Hierarchical Bayesian time series models. In Maximum entropy and Bayesian methods (pp. 15-22). Springer Netherlands.

Berthier, E., Schiefer, E., Clarke, G. K., Menounos, B., and Rémy, F. (2010). Contribution of Alaskan glaciers to sea-level rise derived from satellite imagery. Nature Geoscience, 3(2), 92-95.

Bhatia, M. P., Das, S. B., Kujawinski, E. B., Henderson, P., Burke, A., and Charette, M. A. (2011). Seasonal evolution of water contributions to discharge from a Greenland outlet glacier: insight from a new isotope-mixing model. Journal of Glaciology, 57(205), 929-941.

Brown, G. H., Tranter, M., and Sharp, M. J. (1996). Experimental investigations of the weathering of suspended sediment by alpine glacial meltwater. Hydrological Processes, 10(4), 579-597.

Buttle, J. M. (1998). Fundamentals of small catchment hydrology. In Isotope Tracers in Catchment Hydrology, Kendall, C., McDonnell, J.J. (eds). Elsevier: The Netherlands; Page 1-43.

Cable, J., Ogle, K., and Williams, D. (2011). Contribution of glacier meltwater to streamflow in the Wind River Range, Wyoming, inferred via a Bayesian mixing model applied to isotopic measurements. Hydrological Processes, 25(14), 2228-2236.

Chanudet, V., and Filella, M. (2008). Size and composition of inorganic colloids in a peri-alpine, glacial flour-rich lake. Geochimica et Cosmochimica Acta, 72(5), 1466-1479.

Craig, H. (1961), Isotopic variations in meteoric waters, Science, 133(3465), 1702-1703, doi:10.1126/science.133.3465.1702.

Cogley, J. G., Hock, R., Rasmussen, L. A., Arendt, A. A., Bauder, A., Braithwaite, R. J., and Zemp, M. (2011). Glossary of glacier mass balance and related terms, IHP-VII technical documents in hydrology No. 86, IACS Contribution No. 2. International Hydrological Program, UNESCO, Paris.

Cooper, L. W. (1998). Isotopic Fractionation in Snow Cover. Isotope Tracers in Catchment Hydrology, 119.

Coplen, T. B., Neiman, P. J., White, A. B., and Ralph, F. M. (2015). Categorization of northern California rainfall for periods with and without a radar brightband using stable isotopes and a novel automated precipitation collector. Tellus B, 67.

Dahlke, H. E., Lyon, S. W., Jansson, P., Karlin, T., and Rosqvist, G. (2014). Isotopic investigation of runoff generation in a glacierized catchment in northern Sweden. Hydrological Processes, 28(3), 1383-1398.

Dansgaard, W. (1964). Stable isotopes in precipitation. Tellus, 16(4), 436-468.

Faure, G., and Mensing, T. M. (2005). Isotopes. Principles and Applications, 897.

Gillespie, A., and Molnar, P. (1995). Asynchronous maximum advances of mountain and continental glaciers. Reviews of Geophysics, 33(3), 311-364.

Hannah, D. M., Kansakar, S. R., Gerrard, A. J., and Rees, G. (2005). Flow regimes of Himalayan rivers of Nepal: nature and spatial patterns. Journal of Hydrology, 308(1), 18-32.

Ingraham, N. L. (1998). Isotopic variations in precipitation. Isotope Tracers in Catchment Hydrology, 87-118.

Jorgenson, M. T., Yoshikawa, K., Kanevskiy, M., Shur, Y., Romanovsky, V., Marchenko, S., Grosse, G., Brown, J., & Jones, B. (2008). Permafrost characteristics of Alaska. In Proceedings of the Ninth International Conference on Permafrost (Vol. 3, pp. 121-122). University of Alaska: Fairbanks.

Kendall, C., and Caldwell, E. A. (1998). Fundamentals of isotope geochemistry. Isotope tracers in catchment hydrology, 51-86.

Kido, D., Chikita, K. A., and Hirayama, K. (2007). Subglacial drainage system changes of the Gulkana Glacier, Alaska: discharge and sediment load observations and modelling. Hydrological Processes, 21(3), 399-410.

Klaus, J., and McDonnell, J. J. (2013). Hydrograph separation using stable isotopes: Review and evaluation. Journal of Hydrology, 505, 47-64.

Kong, Y., and Pang, Z. (2012). Evaluating the sensitivity of glacier rivers to climate change based on hydrograph separation of discharge. Journal of Hydrology, 434, 121-129.

La Frenierre, J., and Mark, B. G. (2014). A review of methods for estimating the contribution of glacial meltwater to total watershed discharge. Progress in physical Geography, 38(2), 173-200.

Lemke, P., Ren, J., Alley, R. B., Allison, I., Carrasco, J., Flato, G., and Zhang, T. (2007). Observations: changes in snow, ice and frozen ground.

Liljedahl, A. K., Gädeke, A., O'Neel, S., Gatesman, T. A., & Douglas, T. A. (2017). Glacierized headwater streams as aquifer recharge corridors, subarctic Alaska. Geophysical Research Letters, 44(13), 6876-6885.

Mark, B. G., and Seltzer, G. O. (2003). Tropical glacier meltwater contribution to stream discharge: a case study in the Cordillera Blanca, Peru. Journal of Glaciology, 49(165), 271-281.

Mark, B. G., McKenzie, J. M., and Gómez, J. (2005). Hydrochemical evaluation of changing glacier meltwater contribution to stream discharge: Callejon de Huaylas, Peru. Hydrological Sciences Journal, 50(6).

McNamara, J. P., Kane, D. L., and Hinzman, L. D. (1997). Hydrograph separations in an Arctic watershed using mixing model and graphical techniques. Water Resources Research, 33(7), 1707-1719.

Mook, W.G. ed., (2000). Environmental isotopes in the hydrological cycle: principles and applications; IHP-V. 1. Introduction: theory, methods, review. Unesco.

Ogle, K., Wolpert, R. L., and Reynolds, J. F. (2004). Reconstructing plant root area and water uptake profiles. Ecology, 85(7), 1967-1978.

Ohlanders, N., Rodriguez, M., & McPhee, J. (2013). Stable water isotope variation in a Central Andean watershed dominated by glacier-and snowmelt. Hydrology & Earth System Sciences Discussions, 9(10).

Pu, T., He, Y., Zhu, G., Zhang, N., Du, J., and Wang, C. (2013). Characteristics of water stable isotopes and hydrograph separation in Baishui catchment during the wet season in Mt. Yulong region, south western China. Hydrological Processes, 27(25), 3641-3648.

Radić, V., and Hock, R. (2010). Regional and global volumes of glaciers derived from statistical upscaling of glacier inventory data. Journal of Geophysical Research: Earth Surface, 115(F1).

Raymond, C. F., Benedict, R. J., Harrison, W. D., Echelmeyer, K. A., and Sturm, M. (1995). Hydrological discharges and motion of Fels and Black Rapids Glaciers, Alaska, USA: implications for the structure of their drainage systems. Journal of Glaciology, 41(138), 290-304.

Richey, J. E. (1983). Interactions of C, N, P, and S in river systems: a biogeochemical model. The Major Biogeochemical Cycles and Their Interactions. Wiley, New York, 365-383.

Suecker, J. K., Ryan, J. N., Kendall, C., and Jarrett, R. D. (2000). Determination of hydrologic pathways during snowmelt for alpine/subalpine basins, Rocky Mountain National Park, Colorado. Water Resources Research, 36(1), 63-75.

Taylor, S., Feng, X., Kirchner, J. W., Osterhuber, R., Klaue, B., and Renshaw, C. E. (2001). Isotopic evolution of a seasonal snowpack and its melt. Water Resources Research, 37(3), 759-769.

Taylor, S., Feng, X., Williams, M., and McNamara, J. (2002). How isotopic fractionation of snowmelt affects hydrograph separation. Hydrological Processes, 16(18), 3683-3690.

Tranter, M., Sharp, M. J., Lamb, H. R., Brown, G. H., Hubbard, B. P., and Willis, I. C. (2002). Geochemical weathering at the bed of Haut Glacier d'Arolla, Switzerland—a new model. Hydrological Processes, 16(5), 959-993.

Chapter 1 Glacier contribution to lowland streamflow: A multi-year, geochemical hydrograph separation study in subarctic Alaska[1]

Abstract

Glacier melt affects the geochemical composition of rivers; however, quantifying the glacier contribution to subarctic watershed-scale runoff has attracted limited attention. To estimate glacier contribution, we conducted a 6-year geochemical hydrograph separation study in a geologically heterogeneous glacierized watershed in Interior Alaska. Water samples were collected daily from Jarvis Creek during late April through September. Source waters were collected synoptically each year from rain, snow, baseflow (winter discharge), and the glacier terminus discharge. All samples were analyzed for stable water isotopes and dissolved ion concentrations. Stream surface water samples have large seasonal and inter-annual geochemical variation, however, source waters show distinct chemical signatures allowing the application of a geochemical hydrograph separation model to quantify relative source contribution to lowland streamflow. Considerable inter-annual differences within source water signatures emphasize the importance in informing the model with source waters sampled for each season. We estimated a seasonal average of 35% (20 to 44%) glacier terminus discharge contribution with a daily range of 2 (May) to 80% (September). If glacier contribution was to cease completely, stream discharge would be reduced by 48% and 22% in low and high rainfall summers, respectively. Combined with the documented shrinkage of glaciers, our findings emphasizes the need for further research on glacial wastage effect on subarctic watersheds.

[1] Gatesman, T.A., Liljedahl, A.K., Douglas, T.A., Debolskiy, M.V., and Trainor, T.P.. Glacier contribution to lowland streamflow: A multi-year, geochemical hydrograph separation study in subarctic Alaska. Prepared for submission to Chemical Geology.

1. Introduction

Climate warming has significant implications on physical, biological and social parameters in cryosphere systems (McNamara et al., 1997; Mark and Seltzer, 2003; Hinzman et. al., 2005; Mark and McKenzie, 2007; Liu et al., 2008; Muskett and Romanovsky, 2011). Mountain glaciers have consistently lost mass since the 1850's as a result of climate warming (Lemke et al., 2007; Dyurgerov et al., 2010) and are major contributors to global sea-level rise (Meier 1984; Arendt, et al., 2002; Meier et al., 2007; Dyurgerov et al., 2010; Jacob et al., 2012; Gardner et al., 2013; McNabb et al., 2014). Glaciers, seasonally frozen ground, and permafrost strongly influence the hydrologic regime of cold region rivers (McNamara et al., 1997; Mark et al., 2005; Milner et al., 2009; Muskett and Romanovsky, 2011; Liljedahl et al., 2016, Liljedahl et al.,, 2017). However, there is a gap in knowledge of how hydrology in cryospheric systems is affected both seasonally and biogeochemically by glacial recession (Mark et al., 2005; Milner et al., 2009). Continuous hydrologic and geochemical observations that capture seasonal and interannual variations may be of help to understand the hydrologic regime and seasonal controls of source waters to glacierized catchments (Mark et al., 2005; Milner et al., 2009; Bhatia et al., 2011; Klaus and McDonnell, 2013).

Runoff derived from different sources such as glaciers, baseflow and precipitation contain distinct geochemical signatures (Genereaux and Hooper, 1998; Suecker et al., 2000; Bhatia et al., 2011; Cable et al., 2011; Klaus and McConnel, 2013; La Frenierre and Mark; 2014; Arendt et al., 2015). Chemical end-member hydrograph separation models take advantage of this natural variability to allow estimation of the proportion of water sources within a watershed (Genereaux and Hooper, 1998; Suecker et al., 2000; Bhatia et al., 2011; Cable et al., 2011; Klaus and McConnel, 2013; La Frenierre and Mark; 2014; Arendt et al., 2015). Stable water isotope ratios of heavy to light oxygen ($\delta^{18}O$) and deuterium (δD) can be used as chemical tracers of source waters due to kinetic fractionation during condensation, evaporation, sublimation and melting (Ingraham, 1998; Kendall and McDonnell, 1998; Mark and McKenzie, 2007). Stable isotope ratios can yield information on seasonality as winter precipitation tends to be enriched in heavy oxygen and hydrogen isotopes, while summer precipitation tends to be depleted in heavy oxygen and hydrogen isotopes (Dansgaard, 1964; Cooper, 1998; Ingraham, 1998; Kendall and Caldwell, 1998). Stable water isotope ratios have therefore been effectively used as tracers to track source contributions to runoff (Taylor et al., 2002; Mark and Seltzer 2003; Bhatia et al., 2011; Cable et al., 2011;

Ohlanders et al., 2012; Klaus and McConnel, 2013; La Frenierre and Mark; 2014; Arendt et al., 2015). Geochemical hydrograph separation using stable water isotopes have been used successfully to define snowmelt contribution (McNamara et al., 1997; Suecker et al., 2000; Taylor et al., 2002; Shanley et al., 2002) and contribution to total glacial terminus outflow (Yuanqing et al., 2001; Mark and Seltzer, 2003; Liu et al., 2008; Bhatia et al., 2011; Cable et al., 2011; Ohlanders et al., 2013; Wilson et al., 2016). In addition, variations in isotopic compositions of precipitation and contributing waters can be indicators of climate change and environmental processes (Shanley et al., 1998).

Stable water isotopic measurements coupled with additional geochemical parameters such as ion concentrations can be beneficial to understand glacier processes in relation to watershed hydrology (Maurya et al., 2011). Dissolved ions can be used as signatures of source waters in systems that have high water-rock residence time, such as groundwater, soil pore water and sub-glacier water (Wels et al., 1991; Brown et al., 1996; Langmuir, 1997). Sulfate could be used in geochemical hydrograph separation of glacierized watersheds as sulfide oxidation primarily occurs during water-rock interaction at the glacier bedrock interphase (Brown et al., 1996). Chloride can be used as a tracer of precipitation as there are limited sources of chloride in terrestrial environments and it is nearly unreactive with minerals found in soil and surface waters (Langmuir 1997).

Geochemical hydrograph separation mixing models can refine our understanding of watershed systems to support resource management where data and accessibility are limited (Mark and Seltzer, 2007; Baraer et al., 2009; Kong and Pong, 2012). Information of the relative contribution of source waters can be derived without the typical physical hydrological parameters such as discharge, meteorology or glacier mass balance that can be time-consuming and difficult to measure (La Frenierre and Mark, 2013). Geochemical hydrograph separation can quantify and differentiate source reservoir contribution by using multiple equations to describe water balance components in geologically heterogeneous alpine and glacial catchments (Cable et al., 2011; La Frenierre and Mark, 2013; Arendt et al., 2015). Models integrated with multi-component statistical hydrograph separation, such as Bayesian and Monte Carlo techniques, can account for temporal, special, and chemical variation in data sets (Cable et al., 2011; Arendt et al., 2015).

Research on stable water isotopic measurements coupled with dissolved ion hydrograph separation and continuous discharge techniques is limited in glacial catchments (Cable et al., 2011;

Klaus and McConnel, 2013; Dahlke et al., 2014; Wilson et al., 2016). In addition, there is minimal literature on glacially influenced geochemical hydrograph separation at the watershed scale (i.e. Liu et al., 2008, Cable et al., 2011, and Maurya et al., 2011; Wilson et al., 2016) and/or multi-year continuous data (Wilson et al., 2016). This paper assesses the role of glaciers on streamflow in Jarvis Creek watershed, Interior Alaska, using geochemical hydrograph separation techniques during a 6-year study (2011-2016) with continuous summer season sampling and discharge measurements. Geochemical stream water samples were collected daily to address seasonal variation in glacial contribution. Discharge was recorded at the same location. Synoptic sampling of geochemistry were also collected from snow, rain, baseflow (winter discharge), and glacier terminus runoff. The goal is to quantify glacial, snow, rainfall and baseflow contribution to lowland streamflow using hydrograph separation mixing-model methods constrained with stable water isotopes and dissolved ions. The results will help further our knowledge and understanding of sources and flow paths to subarctic glacial watershed streamflow.

2. Site description

The Jarvis Creek watershed drains 634 km^2 of the north side of the Alaska Range, Interior Alaska (63°40”N, 145°40”E) and is a sub-basin of the Delta, Tanana and Yukon Rivers. The watershed is 3.3% glaciated with an elevation range of 350-2,850 meters. Jarvis Creek flows 64.3 km to the confluence with the Delta River. The up-stream portion of Jarvis Creek is narrow and drains glaciers, whereas the down-stream portion loses gradient and widens into an outwash plain with river terraces several meters high. The watershed has typical subarctic continental climate with semi-arid precipitation (mean annual lowland temperature -0.5°C; 303 mm mean annual lowland precipitation (1971-2000; Shulski and Wendler, 2007), tundra, permanent snowfields, low glacier coverage and discontinuous permafrost (Figure 1). Vegetation consist of black spruce, birch, low bush willow, tundra, taiga, and sedge. The underlying soil system is comprised of silt loam, sandy loam, or gravely loam soil complexes.

The geology of the watershed is diverse and comprised of moraines from multiple glacial advances from the Alaska Range, windblown deposits from glacial comminution and stream erosion. The sub-terrain consists of metasedimentary rocks, metadiorite, augen gneiss and massive sulfide deposits from the Early to mid-Cretaceous Period (Aleinikoff et al., 1987; Pavlis et al., 1993). The down-stream (northern) section of the watershed is underlain by discontinuous permafrost and contains thick deposits of permeable gravel sediments with high hydraulic

conductivities. This section is primarily Tanana Gravels deposited in alluvial fans and braid-plain environments that can be up to 1.2 km thick and contain sandstone and conglomerates with granite plutons (Ridgway et al., 2007). The middle section of the watershed ('highland' Figure 1) is composed of stratigraphic units that contain quartz and granite conglomerate and Birch Creek schist that includes quartzite and mica schist, with rhyolite veins and dikes (Wahrhaftig and Hickox, 1955). The up-stream (southern) section is composed of terminal glacial moraine deposits with low hydraulic conductivities.

Discharge of Jarvis Creek exists primarily during the thaw season between April and November. Spring snowmelt elevate streamflow for one to four weeks in the beginning of the season. A low-flow period is typically encountered in early summer between the end of snowmelt and beginning of glacier melt. Flow decreases drastically in Sep./Oct. when air temperatures cool, ceasing to a low of about ~3 m^3s^{-1} in the foothills in late March (Liljedahl et al., 2017). Measured discharge data from 2015 and 2016 that show that Jarvis Creek is an influent stream where a minimum of 48% and 44% of flow was lost to the underlying lowland aquifer in 2015 and 2016, respectively (Liljedahl et al., 2017). Lowland aquifer water levels near the confluence of Jarvis Creek and Delta River increase rapidly starting in late May – early June and begin to decrease in the fall, totaling up to 13 meters in seasonal water level change (Liljedahl et al., 2017).

Decreased glacier coverage of Jarvis Glacier from 1949 to 2015 is associated with a ~1,600 m retreat of bare-ice front (Liljedahl, et al., 2017). In both 2015 and 2016, specific (area-weighted) annual glacier mass balance of Jarvis Glacier is negative, -1,600 and -2,200 mm respectively (Liljedahl et al., 2017). Neighboring Gulkana Glacier with similar climate regimes has experienced approximately 17% de-glaciation since 1966 (O'Neel et al., 2014). Annual glacier mass balance was found to correlate strongly with streamflow in continental climates (O'Neel et al., 2014).

3. Methodology

3.1 Hydrology measurements

Discharge was measured continuously during the thaw season in Jarvis Creek approximately 1 km above the confluence of Jarvis Creek and the Delta River (64.02°N, -145.73°W, 360 m.a.s.l.; "Lowland" Figure 1) in 2013-2016. Stream water level was measured in 2011-2012, but a limited number of discharge measurements did not allow for calculation of continuous discharge. Discharge measurements were conducted using a StreamPro Acoustic

Doppler Current Profiler (ADCP; Teledyne RD Instruments, Poway, CA) ferried on a tethered trimaran boat during high flows (> 10 m^3s^{-1}) and a portable electromagnetic flowmeter (Marsh McBirney Flow-mate model 2000, HACH Company, Loveland, CO) during lower flows (<10 m $^3s^{-1}$). A discharge-rating curve was calculated in 2014, 2015 and 2016 to describe the discharge-water level relationship. Stream water levels were recorded every 15 minutes using both a vented (CS451, Scientific Campbell, INC. Logan, UT) or non-vented pressure transducers (HOBO U20 Water Level Logger, U20-001- 04, 0-4 m, Onset Computer Corporation, Bourne, MA) together with barometric loggers for compensation (HOBO Micro Station Logger, Onset Computer Corporation, Bourne, MA).

To account for watershed-wide summer precipitation, daily and cumulative precipitation data from two different elevations in Jarvis Creek watershed were collected to depict elevational and temporal precipitation patterns (Figure 1). The lower elevation (389 m.a.s.l.) precipitation was acquired from the Big Delta ("Lowland" Figure 1) meteorological station (Global Historical Climatology Network – Daily (GHCND: USW00026415)). Precipitation at a highland elevation (1030 m.a.s.l.; Easting 561974, Northing 7060795) near the middle of the watershed was recorded using a tipping bucket rain gauge data logger protected by a windscreen (Campbell Scientific Texas electronics TE525MM rain gauge 0.01 in. per tip, Scientific Campbell, INC, Logan, UT; 260-953 Alter-Type Wind Screen for Tipping Bucket Rain Gages, Scientific Campbell, INC. Logan, UT).

Annual snow and glacier water equivalent were measured and used as reference to compare modeled source contribution. Following methods published by Rovansek et al., (1996), annual non-glacier snow water equivalent (SWE) was recorded during synoptic snow sampling surveys at up to 45 sites throughout the watershed. Glacier mass balance from ablation stakes was measured from spring and late summer visits to the glacier (Liljedahl et al., 2017).

3.2 Water sample collection

Water samples were collected from bulk stream water, end-of-winter snow pack, rainfall, baseflow (i.e. winter discharge) and glacier terminus runoff. Analyses included stable water isotope ratios (δD and $\delta^{18}O$) and major ion concentrations (Ca^{2+}, $Mg,^{2+}$ Na^+, K^+, NH_4^+, Cl^-, F^-, SO_4^{2-}, PO_4^{3-}, NO_3^-). These geochemical measurements were used to identify source water chemical signatures and to inform hydrograph separation modeling. Bulk stream samples were collected

from Jarvis Creek approximately 1 km above the confluence (360 m) of Jarvis Creek and the Delta River upstream of the Richardson Hwy Bridge ('lowland' location Figure 1). A time series suite of bulk water samples were collected using a Teledyne ISCO 3700 portable automatic water sampler (Teledyne ISCO, Lincoln, NE). Bulk stream sample collection occurred at 17:00 daily during ice-free conditions in spring to late fall when sampling ceased due to shore ice formation. In addition, samples were collected over five diurnal cycles each July. A total of 201 diurnal cycle stream water samples were collected. The highest diurnal standard deviations for the 6 years were 0.3‰ and 1.7‰ for $\delta^{18}O$ and δD, respectively; therefore, sampling more than once per day was determined to not be necessary. Water samples were collected into 250 mL HDPE bottles (Nalgene, Thermo Fisher Scientific, Inc., Waltham, MA) with 10 mL of mineral oil added to prevent evaporation and any associated isotopic enrichment (Cable et al., 2011, Gazis and Feng, 2004, Ingraham, 1998). The sampler stored up to 24 sample bottles. Samples for major ion and stable water isotopes were collected every two to three weeks and were filtered through 0.45 μm polypropylene media disposable filters (VWR International, Radnar, PA) into 60 mL contaminant-free bottles (HDPE Nalgene, Thermo Fisher Scientific Inc., Waltham, MA) in a laboratory. The filtered samples were stored frozen until they were ready for analysis. Field duplicates and laboratory blanks (ultrapure water with a resistivity of 18.1 MΩ, Barnstead Nanopure, Thermo Scientific, Waltham, MA) were analyzed following identical procedures for the samples.

Baseflow water samples of Jarvis Creek streamflow in the foothills were collected each February or March. Samples were filtered through 0.45 μm polypropylene media disposable filters (VWR International, Radnar, PA) into 60 mL trace metal grade bottles (HDPE Nalgene, Thermo Fisher Scientific Inc., Waltham, MA) and frozen for major ion and stable water isotope analyses.

Rainfall event samples were collected 2011-2016 by the Salcha-Delta Soil and Water Conservation District from their office in Delta Junction, AK. In June 2014, bulk precipitation (2-5 weeks) collection systems that consisted of 1 liter bottle (HDPE Nalgene, Thermo Fisher Scientific Inc., Waltham, MA) and funnel (high-density polyethylene) were deployed at three different elevations (365 m.a.s.l., 840 m.a.s.l., and 1,021 m.a.s.l.) in the Jarvis Creek watershed to account for elevational, temporal and geographic isotopic variability of precipitation. Mineral oil was added to collection systems to prevent evaporation and isotopic exchange following the approach by Cable et al., (2011), Ingraham (1998), and Gazis and Feng (2004).

Synoptic snow samples were collected annually with a 10 cm diameter polyvinyl chloride (PVC) corer with a serrated end. These samples were collected from a variety of locations throughout the watershed and represented the end of winter season snow pack depth (elevation range 524-1,311 m.a.s.l.). Snow cores were thawed in sealed containers in a laboratory environment to prevent any isotopic fractionation due to evaporation (Cooper, 1998) and then filtered through 0.45 μm polypropylene media disposable filters (VWR International, Radnar, PA) into 60 mL trace-metal grade bottles (HDPE Nalgene, Thermo Fisher Scientific Inc., Waltham, MA) and frozen (-18°C; Lee et al., 2010; Ohlanders et al., 2012; Taylor et al., 2001). Snow cores were analyzed to allow for automatic integration chemical composition of stratigraphic layers of the snowpack.

During fall helicopter–borne field campaigns, glacier terminus samples were collected in a 125 mL bottle (HDPE Nalgene, Thermo Fisher Scientific Inc., Waltham, MA) roughly 10 m downstream of Jarvis Glacier terminus. Samples were collected once per year in late August, September or October. Samples were cooled during transportation to laboratory environment where they were filtered to less than 0.45 μm using polypropylene media disposable filters (VWR International, Radnar, PA) and then stored frozen at -18°C.

3.3 Chemical analysis

Stable water isotope values of oxygen and hydrogen were measured using Wavelength-Scanned Cavity Ringdown Spectroscopy on a Picarro L2120i (Sunnyvale, California) at the Geochemistry Laboratory at the U.S. Army Cold Regions Research and Engineering Laboratory on Ft. Wainwright, Alaska. Standards and samples were injected into the analyzer for seven separate analyses. Results from the first four injections were not used to calculate the stable isotope values to minimize internal system memory. Analyses of final three sample injections were used to calculate the mean and standard deviation value for each sample. Values are reported in standard per mil notation. Repeated analyses of SMOW, GISP, and SLAP standards (International Atomic Energy Agency) and laboratory standards from Antarctica, Greenland, Hawaii, Vermont, and Fairbanks were used to calibrate the analytical results. Based on approximately one thousand standards analyzed and duplicate sample analysis, the estimated precision is ±0.5‰ for $\delta^{18}O$ and ±0.2‰ for δD.

Major ion concentrations were quantified on a Dionex ICS-3000 ion chromatograph with an AS-19 anion column and CS-12 cation column (Dionex Corporation Sunnyvale, California) at the Geochemistry Laboratory at the U.S. Cold Regions Research and Engineering Laboratory on Ft. Wainwright, Alaska. The analysis used a gradient method using potassium hydroxide eluent and methanesulfonic acid eluent for the anion and cation analysis, respectively. Operating temperature was at 30°C, system flow rate at 1 mL/min and 10 mL sample injection volume. Calibration of the ion chromatograph was achieved using Chromeleon software (Dionix, Sunnyvale, California) with five laboratory analytical standards. Standards were used throughout the analysis to verify system calibration. Based on previous analytical results we estimate the calculated precision for the analyses is ±5 %.

4. Hydrograph separation

A hydrograph separation model (e.g. Bhatia et al., 2011; Cable et al., 2011; Arendt et al., 2015) using geochemical tracers of $\delta^{18}O$, δD, and SO_4^{2-}:Cl^- was used in this study to quantify relative fractional contribution of end-member sources to streamflow of the Jarvis Creek. The model is based on a forward Monte Carlo approach that is constrained with four end-members and their respected annual chemical signatures. The statistical model allowed for use of probability to determine ranges in results, and allows the system to tease out determinate contributions in addition to using daily streamflow data

End-members consisted of glacier terminus runoff, baseflow (i.e. streamflow collected in late winter at the foothills), rain, and snow. Stream (1,053 samples) and source waters (174 samples) were collected and analyzed for geochemical composition for six years (2011-2016). End-member chemical signatures were defined by the relationships of δD and $\delta^{18}O$ (Figure 2) and SO_4^{2-}:Cl^- and $\delta^{18}O$ (Figure 3). End-member geochemical signatures of the four water sources (glacier, rain, snow, and baseflow) inform the hydrograph separation analysis (Table 1).

We used the following (common) assumptions in our hydrograph separation models (adapted from Buttle, 1998; Cable et al., 2011; La Frenierre and Mark, 2013; Klaus and McDonnell, 2013):

1) End-member signatures are constant throughout time and space, i.e. across the watershed (Cable et al., 2011; Klaus and McDonnell, 2013)

2) Selected chemical tracers are conservative and are not subject to any post mixing chemical change (La Frenierre and Mark, 2013; Klaus and McDonnell, 2013)
3) Water contributions from soil vadose zone to streamflow are negligible (Cable et al., 2011; Klaus and McDonnell, 2013).

We also assume glacier terminus flow consists of glacier surface and subsurface ablation, winter depositional melt and summer precipitation from the entire watershed, i.e. including non-glacierized areas, draining to the glacier terminus. Additional smaller glaciers contribute to Jarvis Creek and we assume their stable isotopic composition being similar to Jarvis Glacier. Glacier samples used in the model were sampled from late August to early October to reduce the effect of elution by the winter snowpack (Brown et al., 1996). The fractional contributions of source waters were assumed to not change across the down-stream section Jarvis Creek, which loses water to the lowland aquifer.

Geochemical hydrograph separation models quantify and differentiate source end-member contribution through multiple equations (La Frenierre and Mark, 2014). Conservative tracers are assumed to mix in proportion to their fractional discharge contribution, leading to the following mass conservation equations specified for our 4 component system:

$$\begin{cases} f_{gl} + f_{bf} + f_{rn} + f_{sn} = 1 \\ C_{gl}^{\delta^{18}O} f_{gl} + C_{bf}^{\delta^{18}O} f_{bf} + C_{rn}^{\delta^{18}O} f_{rn} + C_{sn}^{\delta^{18}O} f_{sn} = S^{\delta^{18}O} \\ C_{gl}^{\delta D} f_{gl} + C_{bf}^{\delta D} f_{bf} + C_{rn}^{\delta D} f_{rn} + C_{sn}^{\delta D} f_{sn} = S^{\delta D} \\ C_{gl}^{SO_4^{2-}:Cl^-} f_{gl} + C_{bf}^{SO_4^{2-}:Cl^-} f_{bf} + C_{rn}^{SO_4^{2-}:Cl^-} f_{rn} + C_{sn}^{SO_4^{2-}:Cl^-} f_{sn} = S^{SO_4^{2-}:Cl^-} \end{cases} \quad (1)$$

The end-members (source waters) in our model include the glacier terminus runoff (*gl*), baseflow (*bf*), rain (*rn*), and snow (*sn*). Superscripts represent chemical tracers including $\delta^{18}O$, δD, and SO_4^{2-}:Cl^-. The fractional contribution to net discharge of the *i*-th end-member ($i \in (1,2,\dots,n)$) is f_j. C_i^j are the tracer concentrations of the *i*-th end-member that contribute to the net stream concentration S^j, where *i* represents end-members, *j* represents chemical tracers ($j \in (1,2\dots,n-1)$), and *n* represents number of end-members in model (Bhatia et al., 2011). In order to solve a system with *n* sources, *n-1* different tracers are needed (Bhatia et al., 2011).

The model used in this study is based on the Forward Monte Carlo approach that estimates the probability of fractional end-member (source water) contributions from an assumed distribution of end-member tracer concentrations and stream concentrations. In addition to major assumptions listed above, the following assumptions are used in this model:

1) There are no more than *4* end-members
2) Each end-member signature is unique (Cable et al., 2011; La Frenierre and Mark, 2013; Klaus and McDonnell, 2013)
3) End-member signatures have normal distribution (Cable et al., 2011).

The system (1) and its solution can be rewritten in matrix form as follows:

$$\begin{bmatrix} 1 \cdots 1 \\ C \end{bmatrix} f = \begin{bmatrix} 1 \\ S \end{bmatrix}$$
$$f = \begin{bmatrix} 1 \\ S \end{bmatrix} \begin{bmatrix} 1 \cdots 1 \\ C \end{bmatrix}^{-1} \qquad (2)$$

Using a Monte Carlo approach, each element of C is determined based on the normal distribution of the measured mean and standard deviation of the tracer concentration sample set of each end-member (glacier terminus, baseflow, rain, and snow) (Cable et al., 2011). Each elements of S is determined based on the normal distribution of daily stream tracer concentrations with standard deviation of either instrument error (stable water isotopes) or error of propagation (SO_4^{2-}:Cl^-) that includes concentrations and instrument error for chloride and sulfate. System (2) is solved repeatedly ($N = 10^6$) by iterative sampling of the end-member and stream tracer concentrations. For each day (i.e. a given set of S's), M matrixes of C and M vectors of S are accepted when the solution of equation (2) meets the following conditions:

$$\begin{cases} 0 \le f_1 \le 1 \\ \vdots \\ 0 \le f_n \le 1 \end{cases} \qquad (3)$$

These inequalities are added to system (2) to enforce the assumption that there are no greater then n end-members so the resulting sample is populated only by solutions that fulfil these inequalities. If the number of attempts in the iterative sampling to get one element in the sample is larger than a presumed threshold $\left((N_{thresh} = 10^3)\right)$ then it is excluded from the solution sample since the assumption of n end-members is too strong. By solving (2) and (3) we obtain a sample of N arrays

of n numbers to estimate probability distribution of end-members' fractional contributions to the stream. The acceptance rate ($\frac{N}{M}$) is used as a proxy for likelihood of the assumption that there are no greater then n end-members in the system. The mean of each probability distribution is used as the estimated fractional contribution to stream flow. The standard deviation calculated from the normal distribution of the probability distribution represents the range in probability in fractional contribution in this hydrograph separation model and shown as error bars in Figures 4c-9c.

5. Results

5.1. Hydrology

Table 2 shows cumulative rainfall, annual snow water equivalent (SWE), and annual glacier mass balance. Higher elevations generally received higher amounts of rainfall throughout the year except for 2014, where lower elevations received more rainfall. No defined elevational trend was found with annual average SWE measurements. Instead, snow accumulation outside the glacier differs with vegetation type where spruce forest show larger SWE than low-shrub tundra. Years 2012, 2013, and 2016 had the highest average SWE measurements of 121-123 mm, whereas 2011, 2014, and 2015 were 50-80 mm. High rainfall years were not found to be associated with high SWE values. Annual mass balance of Jarvis Glacier is negative 2011-2016 with 2011 having the most negative mass balance of -2,800 mm. In addition, there is little to no accumulation zone on Jarvis Glacier.

Measured stream water levels and discharge show inter-annual and seasonal variation. The timing, duration and intensity of peak flow events vary in regards to snowmelt, rain events, and air temperature (Figure 4d-9d). Well-defined peaks in stream water level and discharge during snowmelt season (April-May) occurred in 2012, 2013, 2015, and 2016 where 2013 showed the most defined snowmelt peak. Larger peaks throughout the six years are primarily associated with late summer rainfall events, which were recorded at lowland and/or high elevation meteorological stations. Discharge generally increased mid-late season (June-July) and decreased mid-late September all years. Discharge remained through the winter at the highland site but ceased completely by late October at the lowland site. Aufeis formation in the lowland portion causes overland flooding of Jarvis Creek during spring snow melt. The Salcha-Delta Soil and Water Conservation District ripped the aufeis in 2012 and 2013 to prevent overland flooding and therefore manually diverted the snowmelt water to the downstream discharge monitoring site.

5.2. Chemistry

The covariance between $\delta^{18}O$ and δD of precipitation of Jarvis Creek watershed (2011-2016; n = 296) represents the Local Meteoric Water Line (LMWL; Appendix C.):

$$\delta D = 7.0‰\ \delta^{18}O - 18.2‰ \quad (4).$$

Average end-member signatures for snow, glacier terminus, baseflow, and rainfall for 2011-2016 are distributed around the LMWL (Figure 2). Rain has the highest standard deviation for all years. Rainfall is distributed on the upper end of the LMWL (enriched in heavy isotopes) and snow on the lower end of the LMWL (depleted in heavy isotopes). Glacier terminus water, baseflow and bulk stream samples are distributed between the rain and snow values. Annual averages of $\delta^{18}O$ range from -28.4‰ to -15.8‰ with a largest variation found in rain (Table 1).

Triangle mixing diagrams of $\delta^{18}O$ and SO_4^{2-}:Cl^- ratios show large inter-annual variations in the spatial mixing space of glacier terminus water, rain, snow, and baseflow (Figure 3). Glacier terminus samples show the highest ratios of SO_4^{2-}:Cl^- (666-2159) whereas baseflow samples have similar values to bulk streamflow samples in each year. Both snow and rainfall samples have low SO_4^{2-}:Cl^- ratios (0.8-8.3). Snow samples are depleted in heavy isotopes (-28.4 to -23.4 for $\delta^{18}O$, -219.2 to -178.4 for δD) and rainfall samples are isotopically enriched (-20.9 to -15.8 for $\delta^{18}O$, -160.0 to -133.1 for δD). Bulk streamflow samples are concentrated inside the mixing space concluding that it is credible to use these annual average geochemical signatures for hydrograph separation (Table 1). There are select bulk streamflow samples that fall outside of the triangular mixing space. Most of the samples were collected on either abnormally higher air temperature and/or days with high rainfall at high elevations.

There is seasonal and inter-annual variability in geochemical measurements of bulk streamwater (Figures 4d-9d). Seasonal variation in water $\delta^{18}O$ isotope ratios decrease during the spring which is associated with increased discharge in 2011, 2012, and 2013 (Figures 4d, 5d, and 6d). There are select times throughout the season in 2012 and 2016 where $\delta^{18}O$ values are elevated (isotopically enriched in heavy isotopes relative to average stream ratio) and these times are associated with peaks in discharge and rainfall (Figures 5d and 9d). Stable isotopic values generally increase in mid-June in 2012 and 2013 (Figures 5d and 6d). The dissolved SO_4^{2-}:Cl^- ratio generally increased starting in June/July and decreased mid-to-late September. An increase in SO_4^{2-}:Cl^- ratio in mid-September 2014 is associated with a discharge peak and increased air

temperature (Figure 7d). In 2015, increased SO_4^{2-}:Cl^- ratios are associated with lower discharge measurements and decreased SO_4^{2-}:Cl^- ratios are associated with discharge peaks and rain events (Figure 8d).

5.3. Hydrograph separation

The fractional contribution of baseflow, glacier terminus runoff, rain, and snow to lowland streamflow were estimated in 2011-2016 (Figures 4c-9c). Well-defined snow signals were found in 2012, 2013, and 2015 (Figures 5c, 6c, and 8c) with the greatest snow signal in 2013 (65%). For all six years the glacier terminus contribution generally increased in late June to early July (>40%) and continued to increase (<80%) until the end of the season (Figures 4c-9c). However, baseflow dominated during the majority of the season (38%) in 2016 when glacier contribution peaked at 41% (Figure 9c). Both snow and rain contribution generally decreased (from 26 to 12%) starting in late June to early July for all six years. Only 2012 and 2015 showed defined peaks in rain contribution (36% and 44%), but were not generally associated with rainfall events at the two meteorological stations (Figures 5a, c and 8a, c).

In general, the largest contributor to streamflow was glacier runoff followed by baseflow. The glacier terminus contribution 6-year average is 35% and ranges from 20% (2016) to 44% (2014) with a daily range of 2% (May) to 80% (September) (Table 3). An exception was in 2012 when the highest contribution was in July. Baseflow contribution six-year average was 32% with a range of 26% (2013) to 38% (2016). The maximum baseflow contributions are in July/August (2011-2016). Average annual rain contribution was (16% (2011-2016) and ranged from 9% (2013) to 21% (2016). Average annual snow contribution (17%, 2011-2016) ranged from 13% (2012 and 2014) to 24% (2013).

6. Discussion

6.1. Stable water isotopes

There is inter-annual variation in precipitation isotopic values that may be attributed to differences in precipitation patterns, i.e. atmospheric circulation. For example, 2014 rainfall was an anomaly in total rainfall and also in its rainfall isotopic ratios. Of the six years recorded, higher elevations generally received more rainfall than lower elevations (Table 2; Figures 4b-9b). In contrast, lower elevations received more rainfall than higher elevation in 2014 (Table 2; Figure

7b). The average rainfall isotopic content in 2014 was generally more depleted in heavy isotopes than the other years suggesting that or air masses originated from an a-typical path (Figure 7d; Figures 4d-9d). Typically, low-pressure systems in Interior Alaska originate from south of the Alaska Range and moisture is lost through orographic storms as it passes the range causing increased precipitation at higher elevations in the Jarvis Creek watershed. In 2014, a low-pressure system and moisture originated from the north-west in the lowland Tanana River basin causing more precipitation at lower elevations.

The unique differences in the chemical signatures of rain, snow, baseflow, and glacier melt allow us to use the average isotopic ratio as end-member signatures in hydrograph separation. We found that the bulk streamflow samples, baseflow and glacier terminus water distribute in the middle of the line suggesting a mixing of both rain and snow (Figure 2). Typically snow and glacier melt end-members are similar (Cable et al., 2011; Liu et al., 2008), however, glacier melt end-members from Jarvis have higher $\delta^{18}O$ ratios than snow suggesting a high input of summer precipitation (from the current and prior year) into glacier storage. Furthermore, most of the glacier melt samples are plotted above the LMWL suggesting a higher kinetic fractionation effect during evaporation in the glacier ice which causes a decrease in evaporation. Glacier terminus and baseflow have similar isotopic signatures; therefore, dissolved ion content is used for differentiation.

6.2. Dissolved ions

The select bulk streamflow samples that fall outside of the mixing diagram space in 2012, 2014, and 2015 (Figure 3) coincide with days that have abnormally high air temperatures or high rainfall suggesting that glacier melt and subglacial chemical erosion in increased thus causing the stream signature to fall outside of the normal triangular mixing space. The tributary drainage of McCumber creek to Jarvis Creek may have contributed unique signals from surface water or groundwater contributions. Baseflow samples are also plotted inside the mixing space showing that baseflow is similar to bulk watershed values and that Baseflow is also defined by a mixing of glacier terminus, snow, and rainfall sources as baseflow samples are also plotted inside the mixing space similarly to the bulk streamflow samples.

6.3. Seasonal and inter-annual variation

Seasonal variation of $\delta^{18}O$ isotope ratios of streamflow and end-member signatures can be used as an indicator to suggest the rain, snow, baseflow, and glacier contribution to lowland streamflow. Streamflow during spring snowmelt generally has depleted $\delta^{18}O$ ratios similar to the source snow signatures (Figure 2) compared to the rest of the season (increased ratios suggest rain, decreased ratios suggest snow) (Figure 4d-9d). In addition, the intensity of the snowmelt signal found in the seasonal variation of $\delta^{18}O$ isotope ratios of streamflow agrees well with observed average annual SWE (Table 2; Figures 4d-9d). Seasonal $\delta^{18}O$ variation for 2012 and 2013 show strong snowmelt signals (Figures 5d and 6d), whereas the other years do not (Figures 4d, 7d-9d). Measured average SWE for the watershed was largest in 2012 (121 mm) and 2013 (123 mm) and lower in 2011, 2014, and 2015 (52 to 81 mm) (Table 2). From our meteorological observations, 2011, 2012, and 2013 had low rainfall, whereas 2014, 2015, and 2016 had higher rainfall (Table 2, Figures 4b-9b). In 2012 and 2013, bulk streamflow samples have seasonal variation values depleted $\delta^{18}O$ relative to rain signatures suggesting a lack of rainfall contribution and more contribution from other sources such as baseflow and glacier (Figure 2). Whereas 2014 was a high rainfall summer in the lowlands (average rainfall in the highlands) and the entire season of streamflow had higher $\delta^{18}O$ ratios than baseflow and glacier terminus runoff signatures suggesting a large contribution of summer precipitation (Table 2; Figure 2). The SO_4^{2-}:Cl^- ratios increase in June-July for all six years suggesting an increase in sub-glacial chemical erosion oxidizing sulfide (Figures 4d-9d). Furthermore, there is a decrease in SO_4^{2-}:Cl^- ratios every fall suggesting a reduction in subglacial chemical erosion and glacier melt.

There is an interannual variation in the shape of the SO_4^{2-}:Cl^- and $\delta^{18}O$ mixing diagram spaces due to differences in chemical signatures of source waters from each year as well as bulk streamflow samples. The SO_4^{2-}:Cl^- ratio of glacier terminus water is different each year suggesting that the terminus runoff has different rates of chemical weathering and dilution from snow melt and/or rainfall. Therefore, using a set of geochemical signatures from a single sample set (i.e. one year or one once per year) is insufficient for use in hydrograph separation that span multiple years.

6.4. Hydrograph separation

Hydrograph separation results show high seasonal and inter-annual variation in rain, snow, baseflow, and glacier terminus runoff contribution (Figures 4c-9c). Although there are large uncertainties and ranges in probabilities (0.02%-0.32%), we can observe seasonal and inter-annual linkages between modeled results, geochemical signatures, meteorological data, measured stream discharge and water level (Figures 4-9). The end-member geochemical signatures (SO_4^{2-}:Cl^- and $\delta^{18}O$) of glacier terminus runoff, rainfall, and snow are unique. Baseflow is composed of snow, rain and glaciers. The stable water isotope mixing line (Figure 2) and geochemical triangular mixing diagram (Figure 3) suggest that baseflow does not need to be a fourth end-member in hydrograph separation since the chemical signatures show that baseflow is a mixing of snow, rain, and glacier runoff. Baseflow was ultimately used in the model due to measurable discharge of Jarvis Creek in the highlands during winter months suggesting a baseflow source in the upper reaches of the watershed.

In general, modeled results show high snow and baseflow contribution during spring months (Figures 4c-9c). As the season progresses, there is an increase in glacier contribution and a decrease in snow contribution. In the fall when systems start to freeze, there is a decrease in glacier and rainfall contribution and the system is dominated by baseflow contribution. Although there are similarities in each of the six years studied, results also show different seasonal variation in regards to time, intensity, and duration of spring snowmelt, response to summer rainstorms, influence of baseflow, and duration and intensity of glacier runoff. For example, 2012 and 2013 had higher and longer spring snow melt contribution than the other four years. There was low annual rainfall contribution during low rainfall years (2011-2013) compared to the high rainfall years (2014-2016) (Table 2). Baseflow is generally constant from spring to late summer except in the spring of 2013 when there is high contribution of baseflow in the beginning of spring followed by a sharp decrease (Figure 5c). This could be attributed to a high rainfall event at higher elevation during the fall of 2012 causing an increase in rain-sourced aquifer storage over the winter. Glacier terminus runoff contribution generally increases in June and July (Figures 5c-8c) except in 2011 and 2016 when there is little seasonal variation of glacier contribution (Figures 4c and 9c).

Glacier runoff and baseflow are the dominating sources to annual lowland streamflow (April-September; bed is dry during winter months) in Jarvis Creek watershed (Table 3). It would be expected that baseflow contribution would increase in the spring, decrease in the summer, and

increase in fall. The lowland section of the watershed is losing water to the aquifer and therefore the increased signal in baseflow is not shown. Increased baseflow contribution in 2016 could have been a result of increase rainfall that influenced a flushing of soil water throughout the season resulting in increased baseflow signal in streamflow (Figures 9b, c, d, 3). In 2014, a minimum glacier contribution of 17% was recorded in the spring; this could be attributed to the high glacier contribution estimated in 2013 suggesting high residence time of glacier water in the watershed over the winter months (Table 3; Figures 6c and 7c). Glacier contribution generally increased mid-summer when air temperatures increased above freezing temperatures and decreased in fall when decreasing temperatures ceased the glacier melt and accumulated precipitation as snow (Figures 4a, c- 9a, c).

6.5. Future projections

Glaciers in the sub-arctic have decreased in the last decades and are expected to continue to lose mass in the coming decades. Jarvis Creek future streamflow that is assumed to have a lack of glacier melt runoff can be estimated by using observed data from low (2013) and high rainfall (2016) years. When there is no glacier terminus runoff contribution, lowland stream flow would then be reduced by 48% and 22% flow, in dry and wet years, respectively. Future stream flow will be affected most during July to September when glacier contribution is currently (2011-2016) the dominating source (Figures 10, 11). Future spring flow is not anticipated to be as affected due to its snowmelt contribution.

7. Conclusions

Hydrograph separation shows that Jarvis Creek streamflow is dominated by glacier terminus runoff contribution despite a 3.3% glacier cover within the watershed. Of the six years studied, we estimated an average glacier contribution to lowland streamflow of 35% (20-44%) followed by baseflow at 32% (26-38%). The glacier contribution estimates are conservative as the baseflow is composed of rain, snow, and glacier terminus. Minimum glacier contribution typically occurs in early spring (<25%), and maximum (>50%) is in late summer. Years that showed large modeled spring snowmelt contribution coincided with large measured end-of-winter snow water equivalent. Glacier contribution begins to dominate stream flow beginning in June-July of each year except 2016, which was the wettest year observed. In 2016 year, baseflow contribution dominated the entire season suggesting a flushing of the system due to high rainfall.

Watersheds and communities on the north side of the Alaska Range will be significantly affected by reduced glacier melt by a) lowland aquifer recharge, b) baseflow would come to dominate streamflow. These changes will cause alterations in future stream discharge and flow regimes resulting in a need for different management practices and further research, including hydrogeochemical modeling, on effects of glacial wastage on permafrost degradation. Other studies assume chemical end-member signatures are constant in both time and space (e.g. Mark and McKenzie, 2007, Bhatia et al., 2011). This study shows high inter-annual and seasonal variation in geochemical signatures of sources. This irregularity indicates a need for quality long-term seasonal data sets and multi-year analyses of source waters for effective hydrograph separation studies in refining our understanding of watershed dynamics.

Table 1 *End-member signatures, standard deviations and number of samples (n) collected from Jarvis Creek Watershed for use in hydrograph separation model.*

Year	End-Member	$\delta^{18}O$ (‰)	σ $\delta^{18}O$ (‰)	δD (‰)	σ δD (‰)	SO_4^{2-} : Cl⁻ (μeq L^{-1})	σ SO_4^{2-}/Cl⁻ (μeq L^{-1})	n
2011	Glacier Terminus$^{\tau}$	-22.9	0.1	-173.2	0.9	874.9	61.9	1
	Baseflow	-21.9	1.1	-166.4	7.3	318.2	96.5	7
	Snow	-25.7	2.6	-196.2	20.4	1.0	0.1	9
	Rain	-15.8	4.7	-133.1	31.8	7.2	0.5	8
2012	Glacier Terminus$^{\tau}$*	-21.9	0.1	-165.3	0.8	665.7	47.1	1
	Baseflow	-21.6	0.4	-164.2	2.7	492.8	119.7	5
	Snow	-28.4	1.6	-219.2	11.3	0.8	1.6	15
	Rain	-16.9	3.4	-140.7	20.0	3.5	1.4	7
2013	Glacier Terminus$^{\tau}$	-21.3	0.1	-158.3	0.8	2158.7	152.6	1
	Baseflow	-21.3	0.1	-162.3	0.9	404.4	28.6***	3
	Snow	-25.4	1.7	-198.0	10.6	1.2	1.7	9
	Rain	-18.0	3.0	-143.2	20.0	8.3	28.6	16**
2014	Glacier Terminus$^{\tau}$	-22.1	0.1	-164.3	0.8	916.7	45.8	1
	Baseflow	-21.4	0.1	-162.4	1.2	1064.8	611.8	4
	Snow	-24.3	2.3	-187.5	17.9	1.0	0.9	9
	Rain	-20.9	2.2	-160.0	13.8	4.1	2.8	5
2015	Glacier Terminus$^{\tau}$	-21.3	0.1	-158.7	0.8	1297.5	91.7	1
	Baseflow	-21.5	0.1	-163.5	0.2	1037.9	591.5	6
	Snow	-23.4	2.0	-178.5	13.5	1.9	1.2	12
	Rain	-18.2	1.8	-144.1	12.3	4.1	1.7	11
2016	Glacier Terminus$^{\tau}$	-21.0	0.1	-156.0	0.8	1836.3	129.8	1
	Baseflow	-21.1	0.3	-162.2	0.8	1190.7	556.5	5
	Snow	-24.0	1.9	-182.4	14.2	0.8	0.6	24
	Rain	-18.5	2.7	-146.4	21.2	1.7	1.3	13

$^{\tau}$ Glacier terminus samples represent end-of-season glacier runoff and the standard deviation represents instrumental error since there is only one sample used for the end-member signature (0.5‰ $\delta^{18}O$ and δD; 0.5% dissolved ions).
σ sample set standard deviation unless otherwise noted
*2012 glacier terminus sample is from mid-season collection because end-of-season showed summer precipitation signal due to high rain event during collection (-18.3‰).
**2013 rain sample ion data and standard deviation was found from averaging rain data from 2011, 2012, 2014, 2015, and 2016
*** Propagation of error used if greater than sample set standard deviation

Table 2 *Cumulative rain, end of winter snow water equivalent, and glacier annual mass balance for Jarvis Creek watershed, 2011-2016. Elevation are as follows: Lowland (389 m.a.s.l.), Highland (840 m.a.s.l.), snow water equivalent (524-1311 m.a.s.l.), glacier mass balance water equivalent (1290-1746 m.a.s.l.).*

	Rain Lowland (mm)	Rain Highland (mm)	End of Winter Snowpack (mm SWE)	Glacier Annual Mass Balance (mm WE)
2011	183	--	67	-2800
2012	184	--	121	-1200
2013	152	313	123	-2000
2014	259	218	52	-1100
2015	211	320	81	-1600
2016	221	426	122	-2200

Table 1 *Estimated annual average and daily minimum and maximum fractional contribution of source waters, baseflow, glacier, rain, and snow, of Jarvis Creek watershed, 2011-2016, as determined by geochemical hydrograph separation techniques.*

Year	Source	Annual Average	Daily Minimum	Daily Maximum
2011	Baseflow	34%	10%	47%
	Glacier	30%	2%	76%
	Rain	20%	11%	37%
	Snow	16%	3%	53%
2012	Baseflow	32%	12%	49%
	Glacier	44%	6%	76%
	Rain	11%	3%	36%
	Snow	13%	2%	50%
2013	Baseflow	26%	6%	55%
	Glacier	41%	3%	80%
	Rain	9%	3%	30%
	Snow	24%	3%	65%
2014	Baseflow	27%	17%	51%
	Glacier	41%	17%	64%
	Rain	19%	7%	50%
	Snow	13%	5%	33%
2015	Baseflow	34%	22%	63%
	Glacier	33%	15%	55%
	Rain	18%	7%	44%
	Snow	15%	6%	33%
2016	Baseflow	38%	23%	46%
	Glacier	20%	10%	41%
	Rain	21%	9%	39%
	Snow	20%	7%	41%

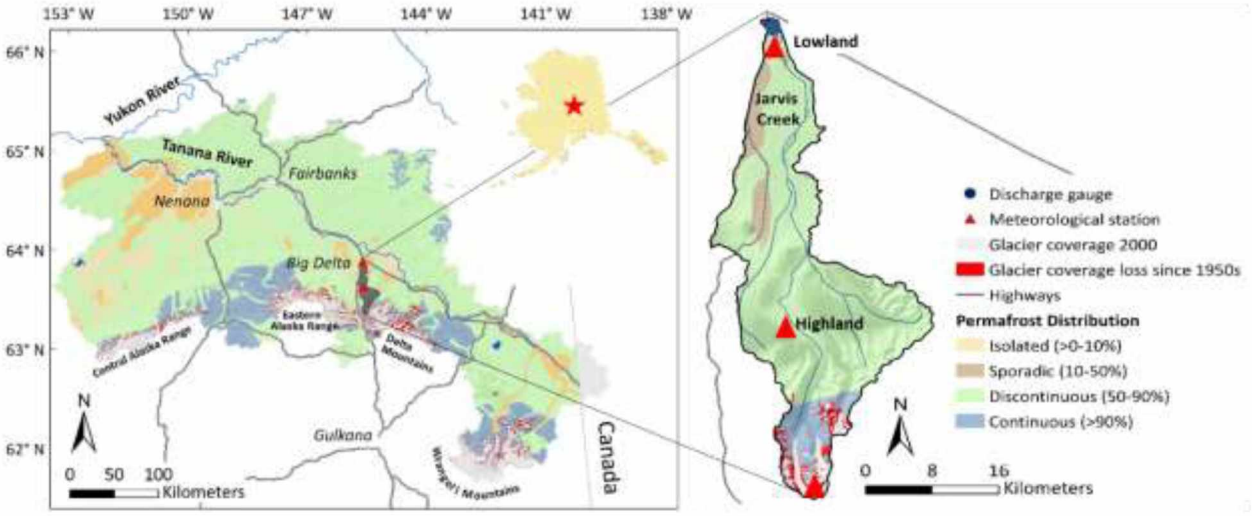

Figure 1 *Jarvis Creek watershed (634 km^2) is a sub-basin of the Tanana and Yukon Rivers. Jarvis Creek watershed is 3.3% glacierized. It has typical subarctic land features that include discontinuous permafrost, glacier till, tundra, taiga and permanent snowfields (Jorgenson et al., 2008). Discharge gauging stations are denoted with a blue circle and meteorological stations are denoted with a red triangle.*

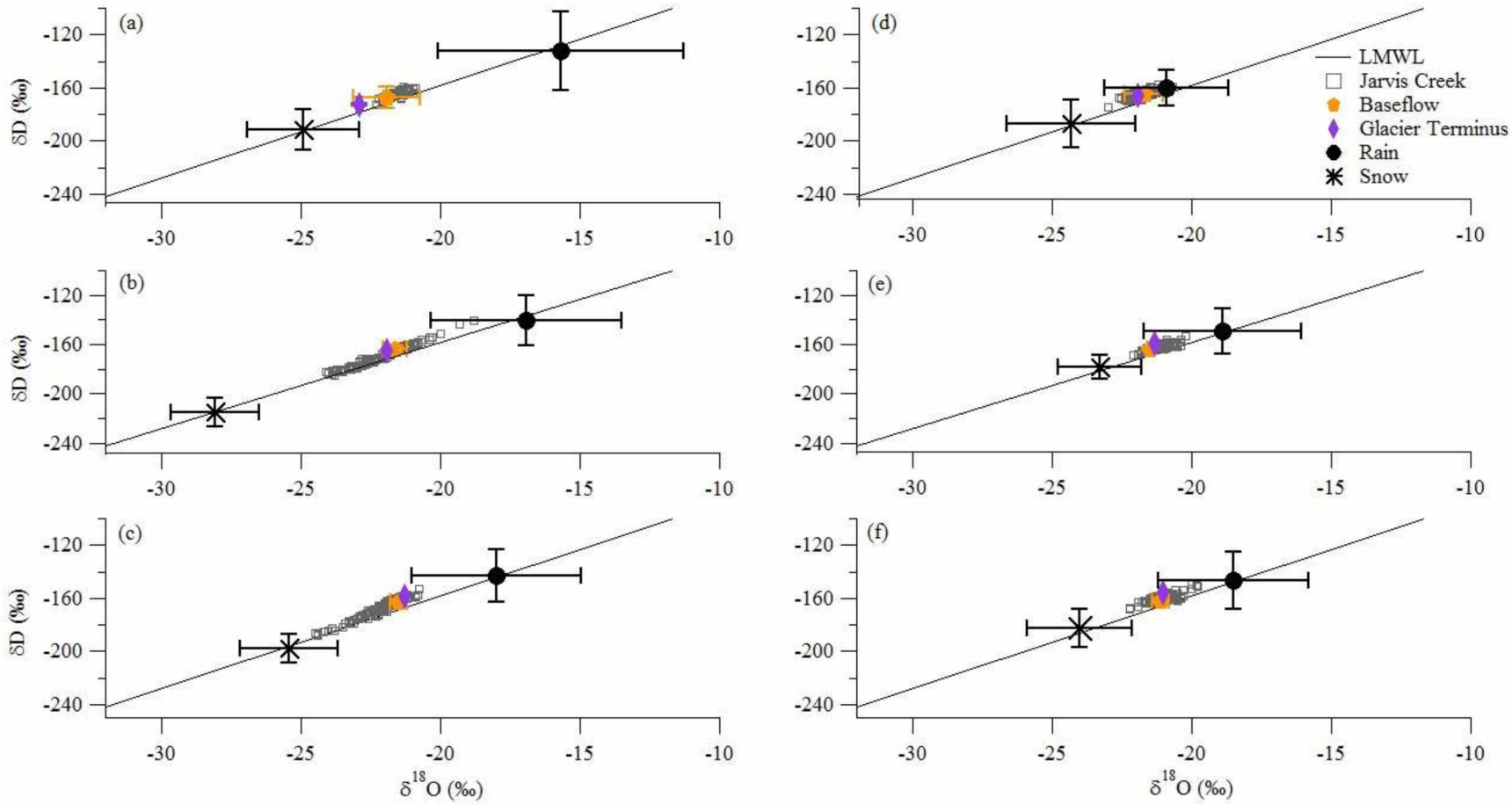

Figure 2 *Isotopic mixing lines of $\delta^{18}O$ and δD for Jarvis Creek Watershed for years 2011 (a), 2012 (b), 2013 (c), 2014 (d), 2015 (e), and 2016 (d). Black line is the LMWL and represents the mixing space of the end-members of glacier terminus, rain and snow. End-member values represent annual averages, which inform the hydrograph separation modeling for respective year. Standard deviations shown in black bars (Table 1). Jarvis Creek are streamflow water samples.*

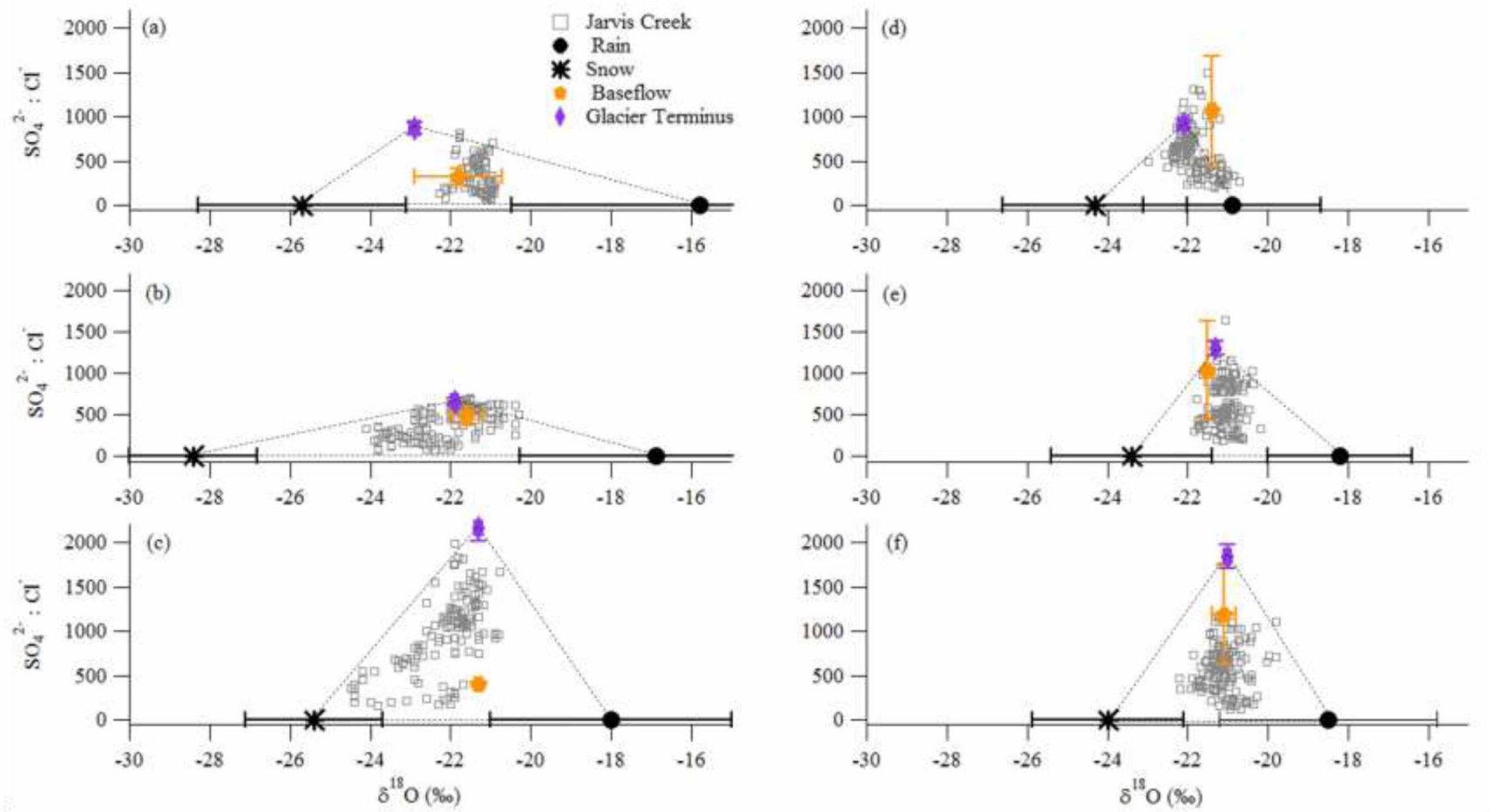

Figure 3 *Triangular mixing diagrams of $\delta^{18}O$ and SO_4^{2-} : Cl^- for Jarvis Creek watershed for years 2011 (a), 2012 (b), 2013 (c), 2014 (d), 2015 (e), and 2016 (d). Dotted black line represents the mixing space of the end-members of glacier terminus runoff, rain and snow. End-member values represent annual averages, which inform the hydrograph separation modeling for respective year. Standard deviations are shown in black bars (Table 1). Jarvis Creek are streamflow water samples.*

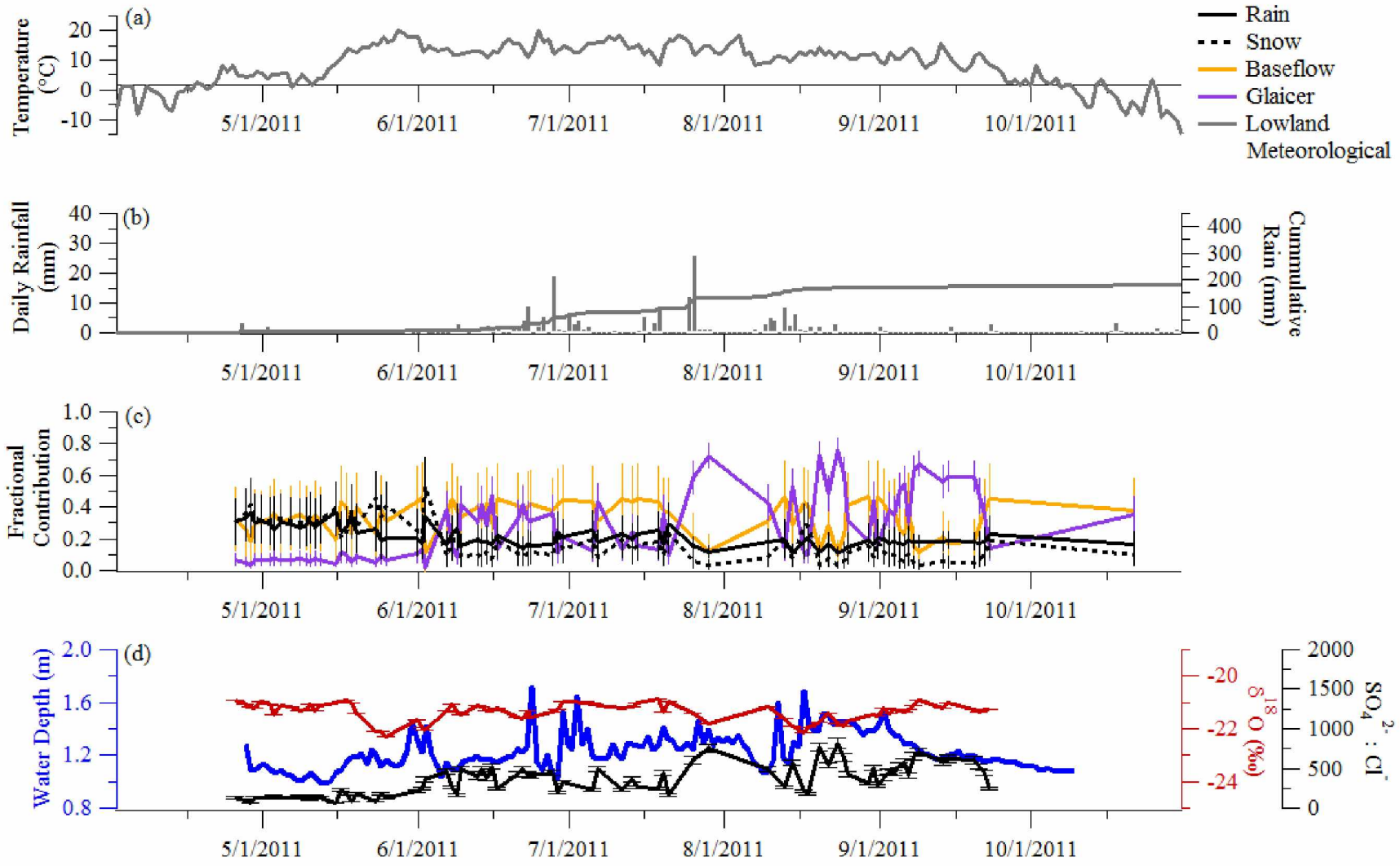

Figure 4 *2011 measured (a) temperature, (b) rainfall, (c) estimated fractional contribution, and (d) stream water depth, $\delta^{18}O$, and SO_4^{2-} : Cl^-. Mean daily air temperature and precipitation measurements were recorded at lowland (389 m.a.s.l.). Estimated fractional contribution values were calculated using hydrograph separation techniques, error bars represent range in probability. Stream discharge measurements and chemistry samples were collected near the confluence of Jarvis Creek and Delta River (360 m.a.s.l.; Figure 1), error bars represent instrumental ($\delta^{18}O$) and propagation (SO_4^{2-}:Cl^-) errors.*

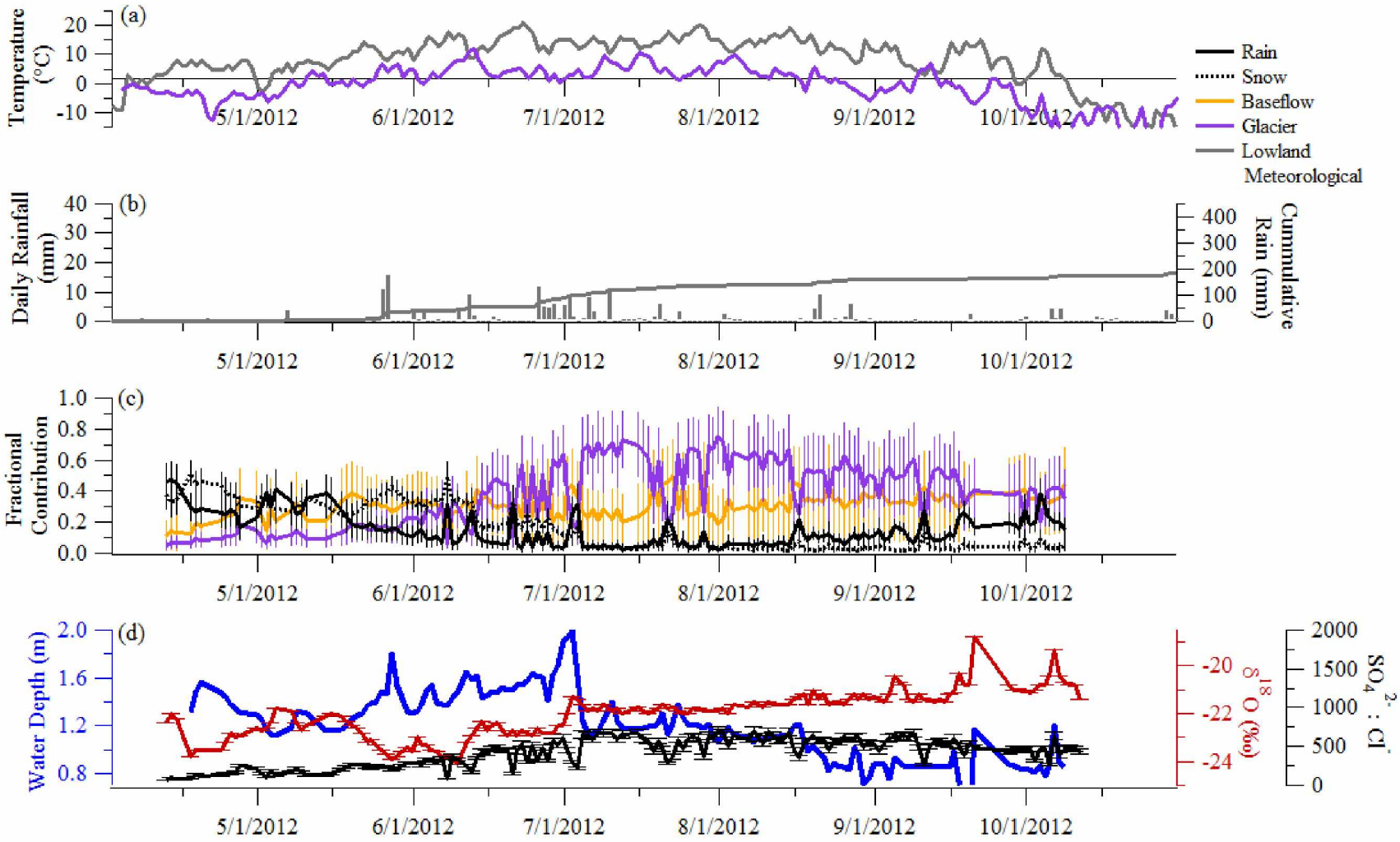

Figure 5 *2012 measured (a) temperature, (b) rainfall, (c) estimated fractional contribution, and (d) stream water depth, $\delta^{18}O$, and SO_4^{2-} : Cl^-. Mean daily air temperature and precipitation measurements were recorded at lowland (389 m.a.s.l.) and Jarvis Glacier (1746 m.a.s.l.) meteorological stations. Estimated fractional contribution values were calculated using hydrograph separation techniques, error bars represent range in probability. Stream discharge measurements and chemistry samples were collected near the confluence of Jarvis Creek and Delta River (360 m.a.s.l.; Figure 1), error bars represent instrumental ($\delta^{18}O$) and propagation (SO_4^{2-}:Cl^-) errors.*

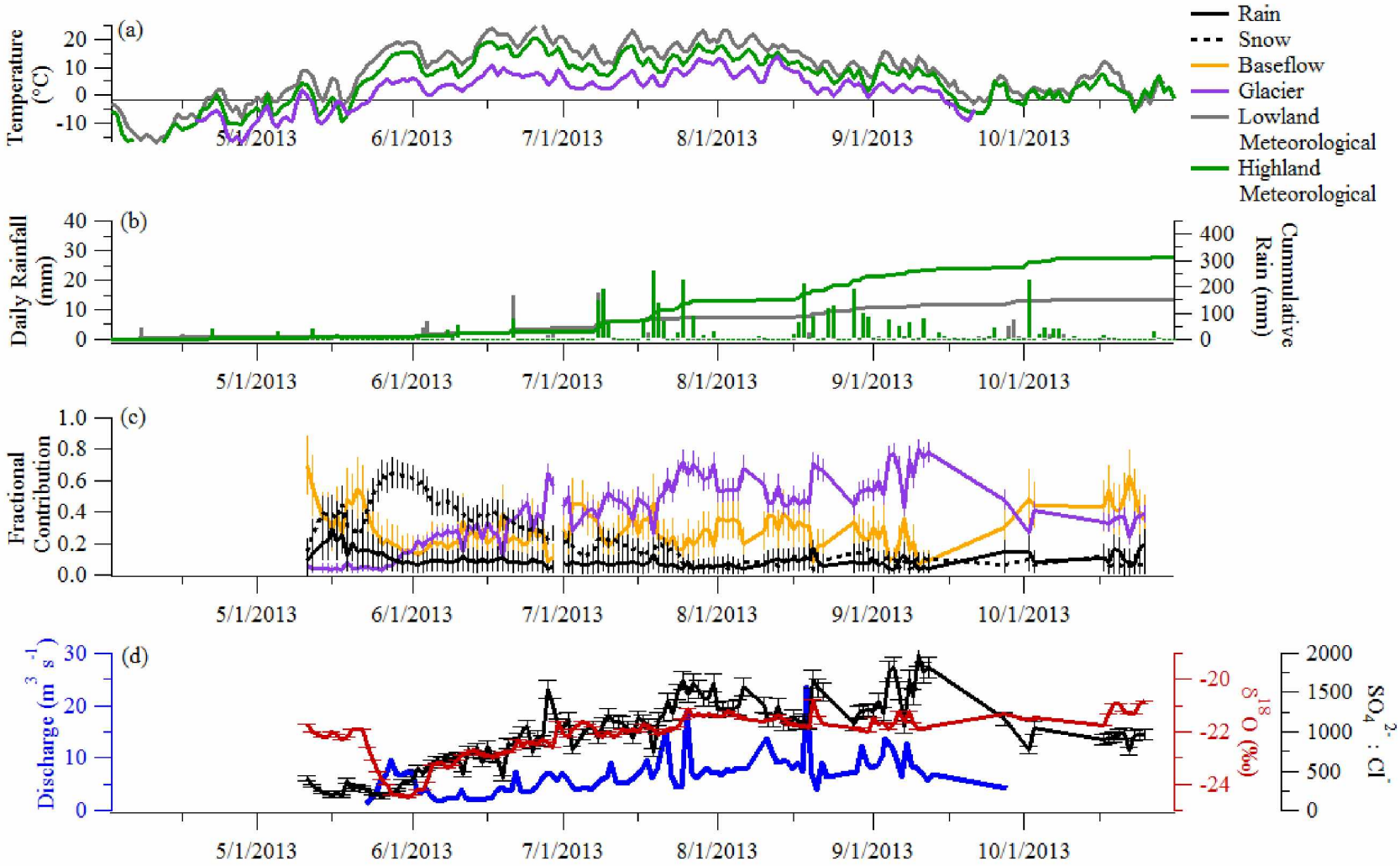

Figure 6 *2013 measured (a) temperature, (b) rainfall, (c) estimated fractional contribution, and (d) discharge, $\delta^{18}O$, and SO_4^{2-} : Cl^-. Mean daily air temperature and precipitation measurements were recorded at lowland (389 m.a.s.l.), highland (840 m.a.s.l.) and Jarvis Glacier (1746 m.a.s.l.) meteorological stations. Estimated fractional contribution values were calculated using hydrograph separation techniques, error bars represent range in probability. Stream discharge measurements and chemistry samples were collected near the confluence of Jarvis Creek and Delta River (360 m.a.s.l.; Figure 1), error bars represent instrumental ($\delta^{18}O$) and propagation (SO_4^{2-}:Cl^-) errors.*

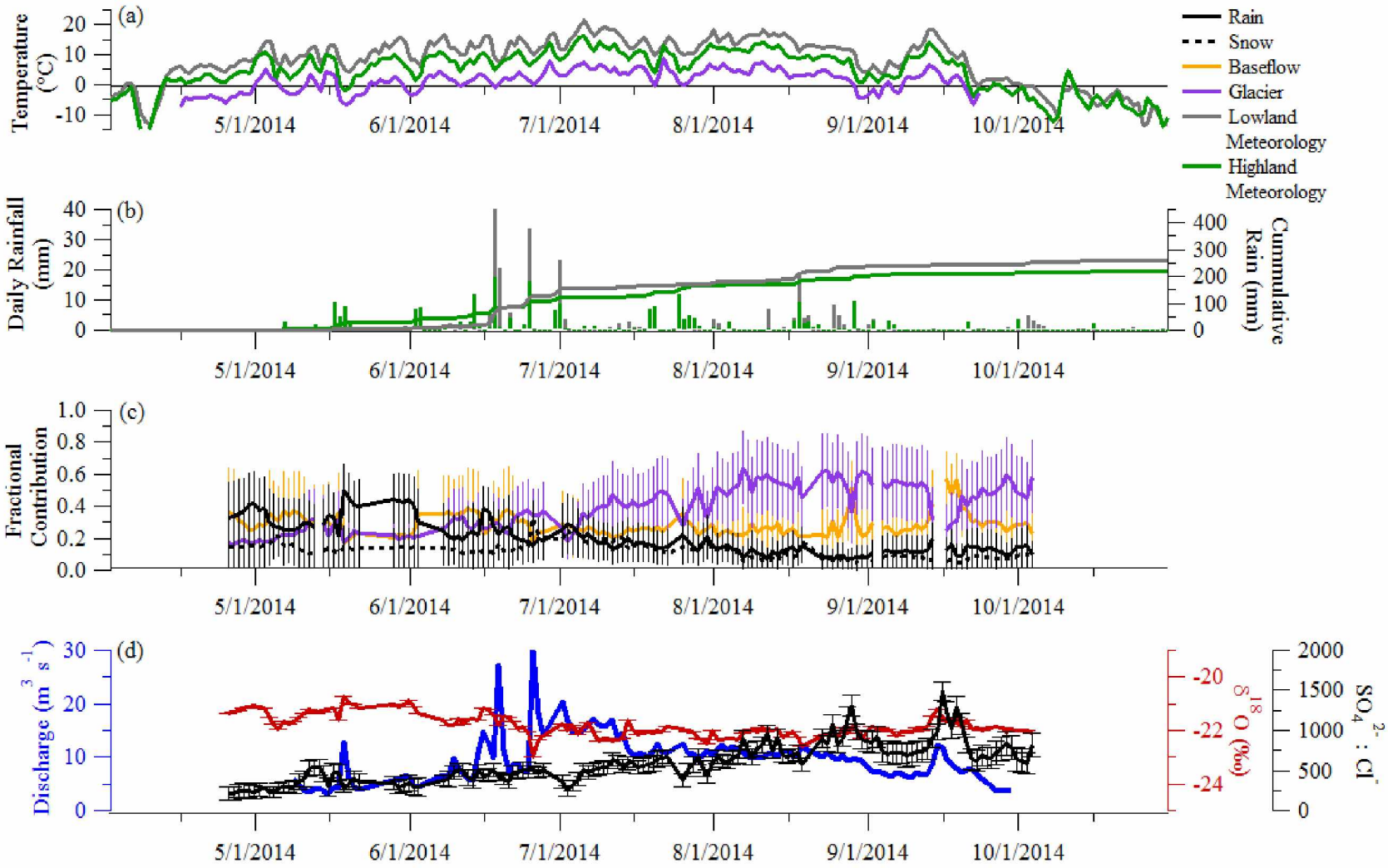

Figure 7 *2014 measured (a) temperature, (b) rainfall, (c) estimated fractional contribution, and (d) discharge, $\delta^{18}O$, and SO_4^{2-} : Cl^-. Mean daily air temperature and precipitation measurements were recorded at lowland (389 m.a.s.l.), highland (840 m.a.s.l.) and Jarvis Glacier (1746 m.a.s.l.) meteorological stations. Estimated fractional contribution values were calculated using hydrograph separation techniques, error bars represent range in probability. Stream discharge measurements and chemistry samples were collected near the confluence of Jarvis Creek and Delta River (360 m.a.s.l.; Figure 1), error bars represent instrumental ($\delta^{18}O$) and propagation (SO_4^{2-}:Cl^-) errors.*

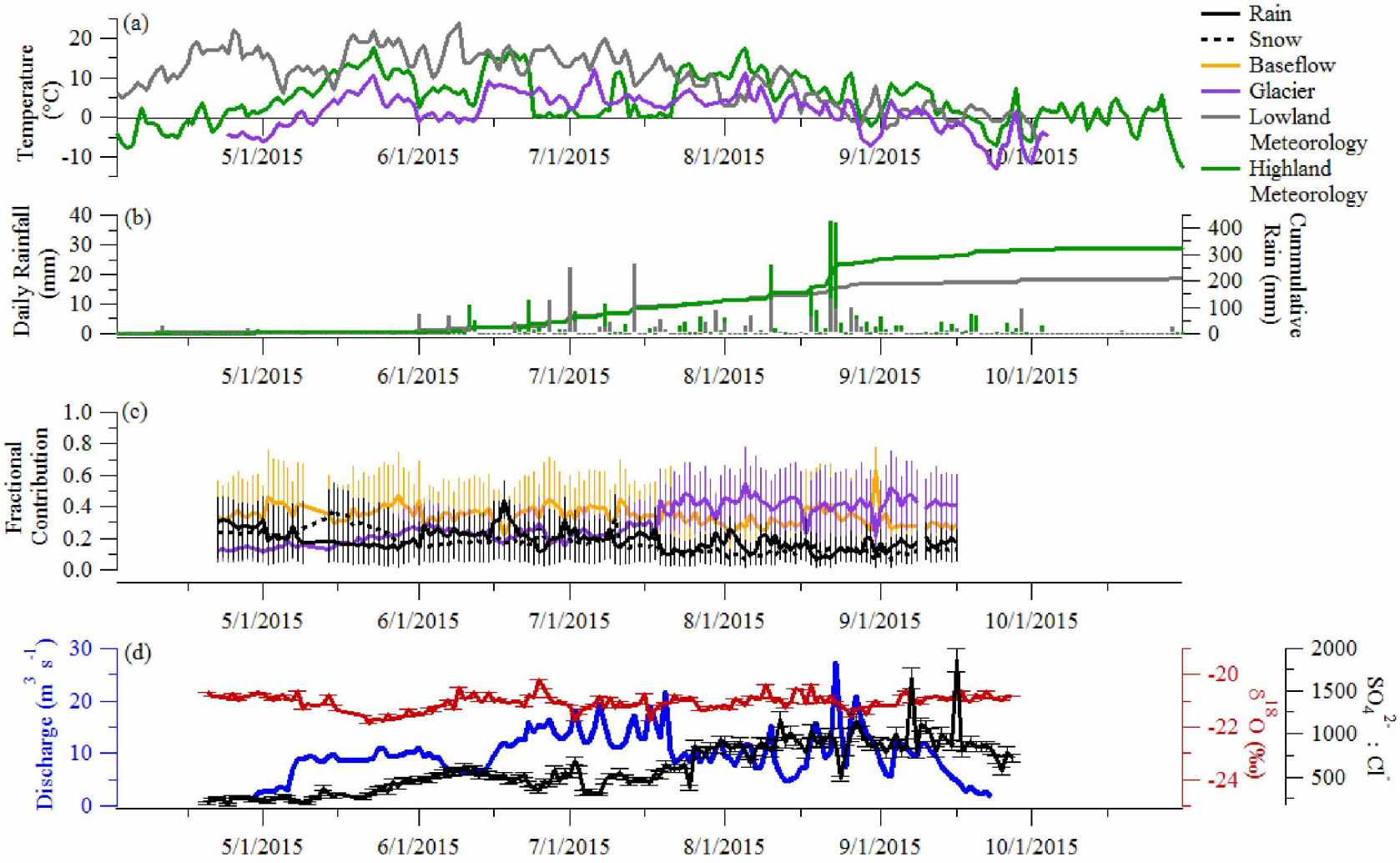

Figure 8 *2015 measured (a) temperature, (b) rainfall, (c) estimated fractional contribution, and (d) discharge, $\delta^{18}O$, and SO_4^{2-} : Cl^-. Mean daily air temperature and precipitation measurements were recorded at lowland (389 m.a.s.l.), highland (840 m.a.s.l.) and Jarvis Glacier (1746 m.a.s.l.) meteorological stations. Estimated fractional contribution values were calculated using hydrograph separation techniques, error bars represent range in probability. Stream discharge measurements and chemistry samples were collected near the confluence of Jarvis Creek and Delta River (360 m.a.s.l.; Figure 1), error bars represent instrumental ($\delta^{18}O$) and propagation (SO_4^{2-}:Cl^-) errors.*

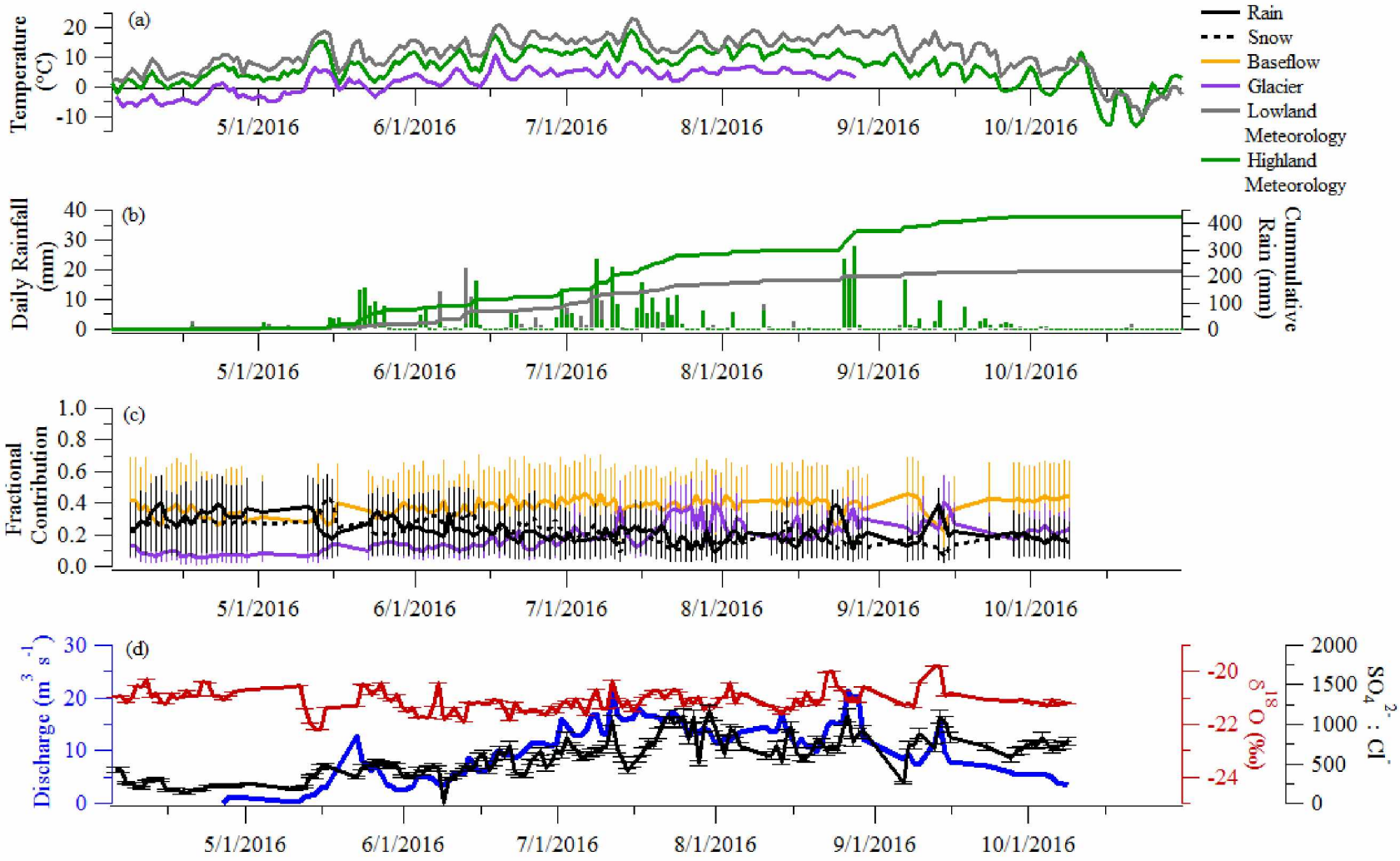

Figure 9 *2016 measured (a) temperature, (b) rainfall, (c) estimated fractional contribution, and (d) discharge, $\delta^{18}O$, and SO_4^{2-} : Cl^-. Mean daily air temperature and precipitation measurements were recorded at lowland (389 m.a.s.l.), highland (840 m.a.s.l.) and Jarvis Glacier (1746 m.a.s.l.) meteorological stations. Estimated fractional contribution values were calculated using hydrograph separation techniques, error bars represent range in probability. Stream discharge measurements and chemistry samples were collected near the confluence of Jarvis Creek and Delta River (360 m.a.s.l.; Figure 1), error bars represent instrumental ($\delta^{18}O$) and propagation (SO_4^{2-}:Cl^-) errors.*

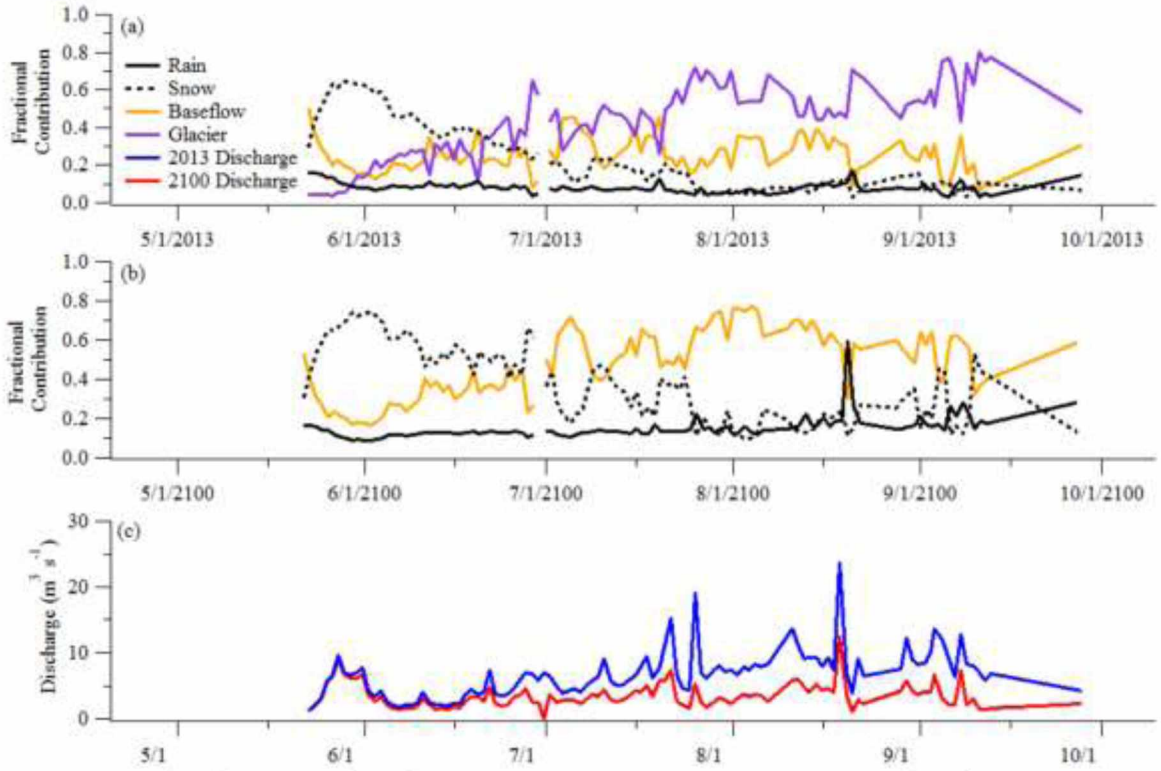

Figure 10. *Current (2013) and projected (2100) source contribution (a, b) and stream runoff (c) of low rainfall year.*

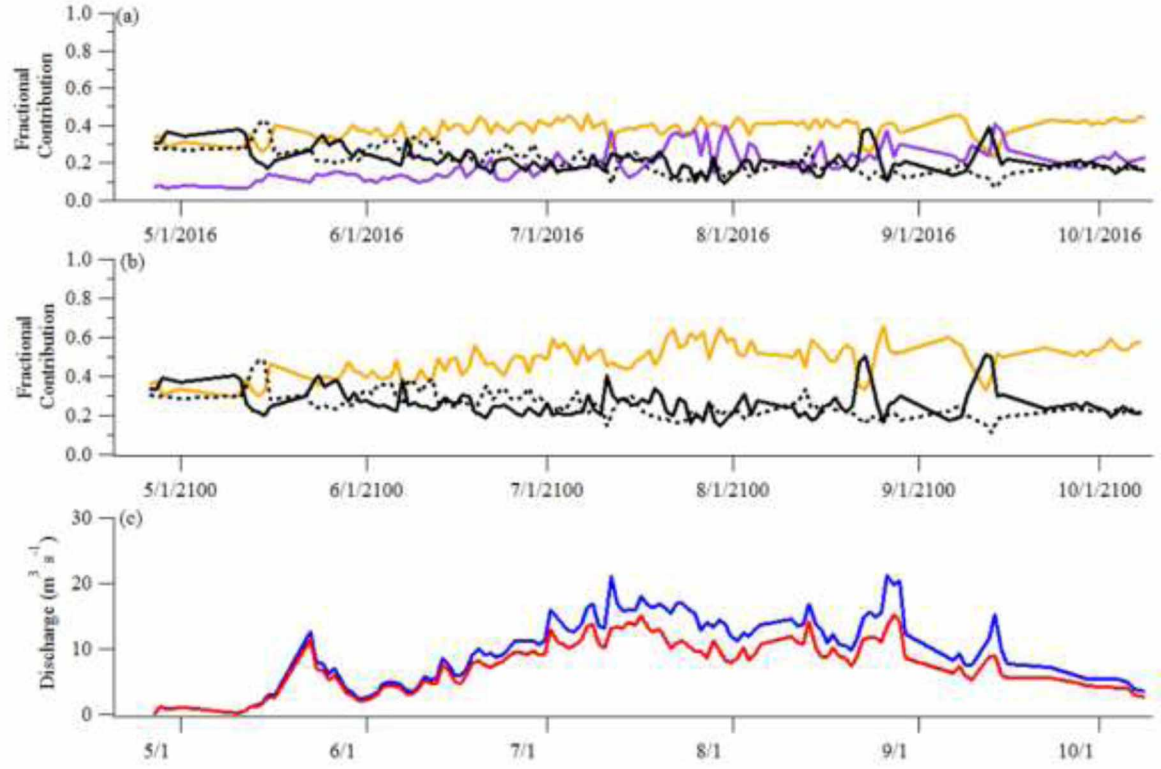

Figure 11. *Current (2016) and projected (2100) source contribution (a, b) and stream runoff (c) of high rainfall year.*

Acknowledgements

We thank Joel Bailey, Amanda Barker, Seth Campbell, Andy Chamberlain, Anne Gaedeke, Art Galvin, Roy Gatesman, Sam Herreid, Regine Hock, Ken Irving, Christian Kleinholz, Aaron Orr, Stephanie Saari, Anna Wagner, Tristian Weiss, Joanna Young, and Salcha-Delta Soil and Water Conservation District for their assistance with field sampling. Aaron Orr and Nikki Jacobs assisted with meteorological data analysis. Anne Gaedeke assisted with development of watershed map. Amanda Barker assisted with reviewing earlier versions of this manuscript.

Funding

This work was supported by the Arctic System Science Program (National Science Foundation, 2013-2016, #1304905), the Department of Defense's Strategic Environmental Research and Development Program (2011-2015, #RC-2110), the Engineer Research and Development Center's Center Directed Research and Army Basic Research (6.1) Programs , Alaska Center for Climate Assessment and Policy (2015), USGS Climate Research and Development program, National Institutes for Water Resources (2012), Alaska University Transportation Center (2012-2013), Alaska Department of Transportation and Public Facilities (2012-2013), and Pacific Northwest Transportation Consortium - PacTrans (2012-2013).

References

Aleinikoff, J. N., Dusel-Bacon, C., Foster, H. L., and Nokleberg, W. J. (1987). Lead isotopic fingerprinting of tectono-stratigraphic terranes, east-central Alaska. Canadian Journal of Earth Sciences, 24(10), 2089-2098.

Arendt, A. A., Echelmeyer, K. A., Harrison, W. D., Lingle, C. S., and Valentine, V. B. (2002). Rapid wastage of Alaska glaciers and their contribution to rising sea level. Science, 297(5580), 382-386.

Arendt, C. A., Aciego, S. M., and Hetland, E. A. (2015). An open source Bayesian Monte Carlo isotope mixing model with applications in Earth surface processes. Geochemistry, Geophysics, Geosystems, 16(5), 1274-1292.

Bhatia, M. P., Das, S. B., Kujawinski, E. B., Henderson, P., Burke, A., and Charette, M. A. (2011). Seasonal evolution of water contributions to discharge from a Greenland outlet glacier: insight from a new isotope-mixing model. Journal of Glaciology, 57(205), 929-941.

Baraer, M., McKenzie, J. M., Mark, B. G., Bury, J., and Knox, S. (2009). Characterizing contributions of glacier melt and groundwater during the dry season in a poorly gauged catchment of the Cordillera Blanca (Peru).

Brown, G. H., Tranter, M., and Sharp, M. J. (1996). Experimental investigations of the weathering of suspended sediment by alpine glacial meltwater. Hydrological Processes, 10(4), 579-597.

Buttle, J. M. (1998). Fundamentals of small catchment hydrology. In Isotope Tracers in Catchment Hydrology, Kendall, C., McDonnell, J. J. (eds). Elsevier: The Netherlands.

Cable, J., Ogle, K., and Williams, D. (2011). Contribution of glacier meltwater to streamflow in the Wind River Range, Wyoming, inferred via a Bayesian mixing model applied to isotopic measurements. Hydrological Processes, 25(14), 2228-2236.

Cooper, L. W. (1998). Isotopic Fractionation in Snow Cover. Isotope Tracers in Catchment Hydrology, 119.

Dahlke, H. E., Lyon, S. W., Jansson, P., Karlin, T., and Rosqvist, G. (2014). Isotopic investigation of runoff generation in a glacierized catchment in northern Sweden. Hydrological Processes, 28(3), 1383-1398.

Dansgaard, W. (1964). Stable isotopes in precipitation. Tellus, 16(4), 436-468.

Douglas, T. A., Wagner, A. M., Walsh, M. E., Gelvin, A.B., Beede, M. C., and Saari, S. P. (2013). Water sampling and groundwater modeling in Donnelly Training Area East, Fort Greely Alaska in FY2013. US Department of Defense, US Army Engineer Research and Development Center Report to U.S. Army Garrison Fort Wainwright Alaska, number 00102895040001.

Dyurgerov, M., Bring, A., and Destouni, G. (2010), Integrated assessment of changes in freshwater 338 inflow to the Arctic Ocean, Journal of Geophysical Research: Atmospheres, 115(D12).

Gardner, A. S., Moholdt, G., Cogley, J. G., Wouters, B., Arendt, A. A., Wahr, J., and Ligtenberg, S. R. (2013). A reconciled estimate of glacier contributions to sea level rise: 2003 to 2009. Science, 340(6134), 852-857.

Gazis, C., and Feng, X. (2004). A stable isotope study of soil water: evidence for mixing and preferential flow paths. Geoderma, 119(1), 97-111.

Genereaux, D. P., & Hooper, R. P. (1998). Oxygen and hydrogen isotopes in rainfall-runoff studies. In Isotope Tracers in Catchment Hydrology, Kendall, C., McDonnell, J. J. (eds). Elsevier: The Netherlands; 839.

Hinzman, L. D., Bettez, N. D., Bolton, W. R., Chapin, F. S., Dyurgerov, M. B., Fastie, C. L., and Yoshikawa, K. (2005). Evidence and implications of recent climate change in northern Alaska and other arctic regions. Climatic Change, 72(3), 251-298.

Ingraham, N. L. (1998). Isotopic variations in precipitation. Isotope Tracers in Catchment Hydrology, 87-118.

Jacob, T., Wahr, J., Pfeffer, W. T. and Swenson, S. (2012). Recent contributions of glaciers and ice caps to sea level rise. Nature 482, 514–518.

Jorgenson, M. T., Yoshikawa, K., Kanevskiy, M., Shur, Y. L., Romanovsky, V., Marchenko, S., Grosse, G., Brown, J., and Jones, B. M. (2008), Permafrost Characteristics of Alaska, Ninth 382 International Conference on Permafrost (NICOP).

Klaus, J., and McDonnell, J. J. (2013). Hydrograph separation using stable isotopes: Review and evaluation. Journal of Hydrology, 505, 47-64.

Kong, Y., and Pang, Z. (2012). Evaluating the sensitivity of glacier rivers to climate change based on hydrograph separation of discharge. Journal of Hydrology, 434, 121-129.

La Frenierre, J., and Mark, B. G. (2014). A review of methods for estimating the contribution of glacial meltwater to total watershed discharge. Progress in Physical Geography, 38(2), 173-200.

Langmuir, D. (1997). Aqueous environmental geochemistry (Vol. 549). Upper Saddle River, NJ: Prentice Hall.

Lee, J., Feng, X., Faiia, A. M., Posmentier, E. S., Kirchner, J. W., Osterhuber, R., and Taylor, S. (2010). Isotopic evolution of a seasonal snowcover and its melt by isotopic exchange between liquid water and ice. Chemical Geology, 270(1), 126-134.

Lemke, P., Ren, J., Alley, R. B., Allison, I., Carrasco, J., Flato, G., Fujii, Y., Kaser, G., Mote, P., Thomas, R.H., and Zhang, T. (2007). Observations: changes in snow, ice and frozen ground. Climate Change 2007: The Physical Science Basis, 337-383.

Liljedahl, A. K., Boike, J., Daanen, R. P., Fedorov, A. N., Frost, G. V., Grosse, G., Hinzman, L. D., Ilijma, Y., Jorgenson, J. C., Matveyeva, N, Necsoiu, M., Raynolds, M. K., Romanovsky, V. E., Schulla, J., Tape, K. D., Walker, D. A., Wilson, C. J., Yabuki, H., and Zona, D. (2016). Pan-Arctic ice-wedge degradation in warming permafrost and its influence on tundra hydrology. Nature Geoscience.

Liljedahl, A. K., Gädeke, A., O'Neel, S., Gatesman, T. A., & Douglas, T. A. (2017). Glacierized headwater streams as aquifer recharge corridors, subarctic Alaska. Geophysical Research Letters, 44(13), 6876-6885.

Liu, Y., Fan, N., An, S., Bai, X., Liu, F., Xu, Z., and Liu, S. (2008). Characteristics of water isotopes and hydrograph separation during the wet season in the Heishui River, China. Journal of Hydrology, 353(3), 314-321.

Mark, B. G., and Seltzer, G. O. (2003). Tropical glacier meltwater contribution to stream discharge: a case study in the Cordillera Blanca, Peru. Journal of Glaciology, 49(165), 271-281.

Mark, B. G., McKenzie, J. M., and Gómez, J. (2005). Hydrochemical evaluation of changing glacier meltwater contribution to stream discharge: Callejon de Huaylas, Peru. Hydrological Sciences Journal, 50(6).

Mark, B. G., and McKenzie, J. M. (2007). Tracing increasing tropical Andean glacier melt with stable isotopes in water. Environmental science and technology, 41(20), 6955-6960.

Maurya, A. S., Shah, M., Deshpande, R. D., Bhardwaj, R. M., Prasad, A., and Gupta, S. K. (2011). Hydrograph separation and precipitation source identification using stable water isotopes and conductivity: River Ganga at Himalayan foothills. Hydrological Processes, 25(10), 1521-1530.

McNabb, R. W., Hock, R., and Huss, M. (2015). Variations in Alaska tidewater glacier frontal ablation, 1985–2013. Journal of Geophysical Research: Earth Surface, 120(1), 120-136

McNamara, J. P., Kane, D. L., and Hinzman, L. D. (1997). Hydrograph separations in an Arctic watershed using mixing model and graphical techniques. Water Resources Research, 33(7), 1707-1719.

Milner, A. M., Brown, L. E., and Hannah, D. M. (2009). Hydroecological response of river systems to shrinking glaciers. Hydrologic Processes. **23**, 62–77.

Meier, M. F. (1984). Contribution of small glaciers to global sea level. Science, 226(4681), 1418-1421.

Meier, M. F., Dyurgerov, M. B., Rick, U. K., O'Neel, S., Pfeffer, W. T., Anderson, R. S., and Glazovsky, A. F. (2007). Glaciers dominate eustatic sea-level rise in the 21st century. Science, 317(5841), 1064-1067.

Muskett, R. R., and Romanovsky, V. E. (2011). Alaskan permafrost groundwater storage changes derived from GRACE and ground measurements. Remote Sensing, 3(2), 378-397.

Ohlanders, N., Rodriguez, M., and McPhee, J. (2013). Stable water isotope variation in a Central Andean watershed dominated by glacier and snowmelt.

O'Neel, S., Hood, E., Arendt, A. L., and Sass, L. (2014). Assessing streamflow sensitivity to variations in glacier mass balance. Climatic Change, 123(2), 329-341.

Pavlis, T. L., Sisson, V. B., Foster, H. L., Nokleberg, W. J., and Plafker, G. (1993). Mid-Cretaceous extensional tectonics of the Yukon-Tanana Terrane, Trans-Alaska Crustal Transect (TACT), east-central Alaska. Tectonics, 12(1), 103-122.

Ridgway, K. D., Thoms, E. E., Layer, P. W., Lesh, M. E., White, J. M., and Smith, S. V. (2007). Neogene transpressional foreland basin development on the north side of the central Alaska Range, Usibelli Group and Nenana Gravel, Tanana basin. Geological Society of America Special Papers, 431, 507-547.

Rovansek, R. J., Hinzman, L. D., and Kane, D. L. (1996). Hydrology of a tundra wetland complex on the Alaskan Arctic Coastal Plain, USA. Arctic and Alpine Research, 311-317.

Shanley, J. B., Pendall, E., Kendall, C., Stevens, L. R., Michel, R. L., Phillips, P. J., Forester, R. M., Naftz, D. L., Beiling Liu, Stern, L., Wolfe, B.B., Page Chamberlain, C. P., Leavitt, S. W., Heaton, T. H. E., Mayer, B., DeWayne Cecil, L., Berry Lyons, W., Katz, B. G., Betancourt, J. L., McKnight, D. M., Blum, J. D., Edwards, T. W. D., House, H. R., Ito, E., Aravena, R. O., and Whelan, J. F. (1998). Isotopes as indicators of environmental change. Isotope tracers in catchment hydrology, Elsevier, Amsterdam, 761-816.

Shanley, J. B., Kendall, C., Smith, T. E., Wolock, D. M., and McDonnell, J. J. (2002). Controls on old and new water contributions to stream flow at some nested catchments in Vermont, USA. Hydrological Processes, 16(3), 589-609.

Shulski, M., and Wendler, G. (2007). The climate of Alaska. University of Alaska Press.

Suecker, J. K., Ryan, J. N., Kendall, C., and Jarrett, R. D. (2000). Determination of hydrologic pathways during snowmelt for alpine/subalpine basins, Rocky Mountain National Park, Colorado. Water Resources Research, 36(1), 63-75.

Taylor, S., Feng, X., Kirchner, J. W., Osterhuber, R., Klaue, B., and Renshaw, C. E. (2001). Isotopic evolution of a seasonal snowpack and its melt. Water Resources Research, 37(3), 759-769.

Taylor, S., Feng, X., Williams, M., and McNamara, J. (2002). How isotopic fractionation of snowmelt affects hydrograph separation. Hydrological Processes, 16(18), 3683-3690.

Wahrhaftig, C., and Hickox, C. A. (1955). Geology and coal deposits, Jarvis Creek coal field, Alaska (No. 989-G).

Wels, C., Cornett, R. J., and Lazerte, B. D. (1991). Hydrograph separation: a comparison of geochemical and isotopic tracers. Journal of Hydrology, 122(1-4), 253-274.

Wilson, A. M., Williams, M. W., Kayastha, R. B., and Racoviteanu, A. (2016). Use of a hydrologic mixing model to examine the roles of meltwater, precipitation and groundwater in the Langtang River basin, Nepal. Annals of Glaciology, 57(71), 155-168.

Yuanqing, H., Theakstone, W. H., Tandong, Y., and Yafeng, S. (2001). The isotopic record at an alpine glacier and its implications for local climatic changes and isotopic homogenization processes. Journal of Glaciology, 47(156), 147-151.

Conclusion

Seasonal and inter-annual variations in stable water isotopes are observed in surface water, precipitation, glacier terminus runoff, and baseflow of Jarvis Creek watershed. Seasonal variation of surface water $\delta^{18}O$ show distinct snowmelt signatures as well as rain and baseflow signatures. Therefore, the seasonal variation is dependent on annual snow pack amount, duration of melt, and rainfall amount as well as glacier and baseflow contribution of each respected year. Rain and snow values are influenced by inter-annual variations of local and regional climatic patterns, which also affect the isotope fractionation of water droplets in storm systems. This, in turn, alters other source water values in the watershed. Dissolved ion composition is not as influenced by climatic patterns as stable water isotopes. However, there is still inter-annual variations in surface water, glacier terminus runoff, and baseflow values. Seasonal and inter-annual variations in geochemistry of the Jarvis Creek watershed contributions shows a need for quality long term water sampling for geochemical hydrograph separation of larger, heterogeneous watersheds.

Hydrograph separation techniques contain many uncertainties in regards to known water sources and their geochemical signatures. Assumptions are used in models to account for major source waters and changes in chemical composition. Minor source waters, such as soil pore water, fog, and intermittent streams, are assumed to be minimal and are not accounted for in modeling techniques. It is also assumed that the chemical composition of source waters or stream surface water do not change. Furthermore, there is inherent error in chemical sampling techniques and sample set deviation, which can further the uncertainty in determining source waters and geochemical signatures of watersheds by methods of hydrograph separation.

Precipitation is highly affected by local climatic patterns causing temporal and spatial variation in rainfall amount and chemical composition. Past studies have shown that using a compilation of precipitation samples to represent a homogenized chemical value of precipitation is deemed acceptable due to mixing in the watershed. However, the use of diverse chemical values to define a chemical signature for end-member modeling causes large uncertainty in modeled results due to the high deviation in sample set values. This technique may be acceptable in small watersheds without high elevational change, but new techniques are necessary to account for precipitation variability in large, heterogeneous watersheds.

In addition, glacier melt and baseflow (groundwater) are not static throughout large watersheds. Therefore, chemical composition of these sources also change throughout the season.

In addition to seasonal variation, there is high inter-annual variation caused by precipitation amount and chemical signatures. Both baseflow and glacier melt can be affected by the amount of rainfall by system flushing during high rain events. Annual snowpack also affects the dynamics of these waters through slow infiltration for baseflow and elution of glacier melt waters.

Hydrograph separation shows that Jarvis Creek watershed is dominated by glacier runoff contribution. Of the 6 years studied, we estimated an average glacier contribution to lowland streamflow of 35% with a minimum of 2%, typically in early spring, and a maximum of 80%, typically in late summer. Years that showed high spring snow melt contribution agreed with stable water isotope signatures, measured discharge of Jarvis Creek, and total annual SWE. Years that had high observed rainfall showed high rainfall contribution as well as low glacier contribution suggesting that rainfall was dominate relative to glacier runoff in those years. Glacier contribution begins to dominate stream flow beginning in June-July of each year except 2016, which was the wettest year observed. This year baseflow contribution was dominate suggesting a flushing of the system due to high rainfall.

Based on climate forecasting and our hydrograph separation results, we expect future stream flow in Jarvis Creek to decrease by 48% in dry years and 22% in wet years by the year 2100. Stream flow will be mostly affected during late season due to lack of glacier contribution to lowland streamflow. Baseflow will become the dominate water source to the watershed, which will also bring concern for future flow in regards to possible permafrost degradation in sub-arctic watersheds.

Appendices

Appendix A. Sediment Crystalline Phases

Stream bed sediment samples were collected at roughly 10 m downstream of the glacier terminus and at the automated water sampling site located about 1 km upstream of the confluence of the Jarvis and Delta Rivers in October 2015. Stream bed sediment samples were passed through a 63 μm sieve and transported to the laboratory where they were dried in an oven at 150°C for 24 hours. Sediment samples were analyzed for crystalline phases by X-Ray Diffraction. An X'Pert PRO Material Research Diffractometer (PANalytical) was equipped with a Cu (Kα λ=1.54060Å) X-ray tube with the generator set at 40 mA and 45 kV. The counting time was set at 85.09 s at a step size of 0.0130° 2θ with scans collected from 5.0078 to 69.9818° 2θ. Diffraction patterns were identified by 2θ of each peak and compared to handbook

Mineral crystal phases of streambed sediments have different intensities at the mouth of the watershed compared to the glacier terminus (Figure A-1., Table A-1.). Streambed sediment collected from the glacier terminus and watershed mouth of Jarvis Creek show similar mineral phases but different intensities. Glacier terminus samples show higher intensity of illite and chlorite minerals than the downstream Jarvis Creek, whereas quartz mineral phase has lower intensity at the glacier terminus. This suggests that illite and chlorite materials are being chemically altered during transport downstream. The higher quartz intensity at the downstream Jarvis Creek could also be attributed to additions of different quartz mineral phases from flow paths through other geology in the downstream portion of the watershed.

When phyllosilicates minerals (illite, chlorite and quartz) are exposed to chemical weathering, potassium, magnesium, aluminum, iron, and silicic acid will be liberated to solution, therefore, these major cations would be a poor tracer for glacier chemical weathering. Sulfur minerals phases were not found in streambed sediment, we can assume the majority of sulfide oxidation is occurring in the Jarvis Glacier bed and sulfate could be used as a tracer for glacier chemical weathering.

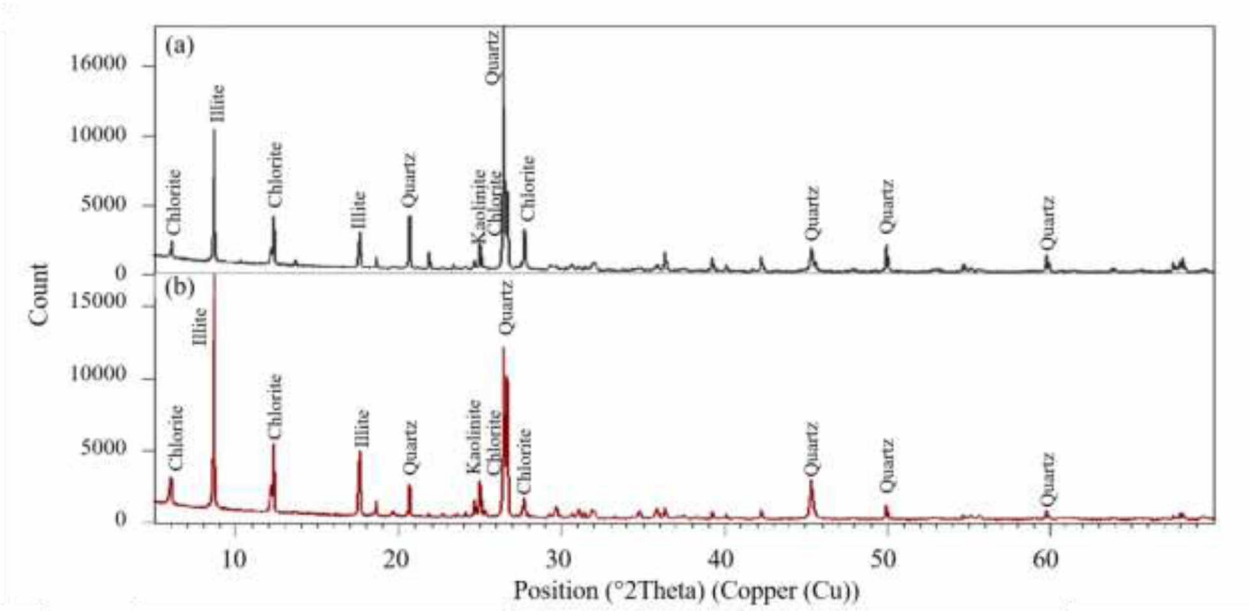

Figure A-1. *Sediment crystalline phases of <63µm bed sediment from Jarvis Creek near mouth (a) and 10 m downstream of glacier terminus (b). Dominate minerals are found in both locations. Jarvis Bridge location tends to have higher intensities of quartz and lower intensities of illite and chlorite (see table 1). There are also trace amounts of kaolinite, feldspar and graphite.*

Table A-1. *Dominant sediment crystalline phases of <63µm bed sediment from Downstream Jarvis Watershed (Jarvis Bridge) and 10 m downstream of glacier terminus (Jarvis Glacier). Dominate minerals are found in both locations. Jarvis Bridge location tends to have higher intensities of quartz and lower intensities of illite and chlorite (see figure 4). There are also trace amounts of kaolinite, feldspar and graphite.*

(Jarvis) Glacier Terminus Sediment				Jarvis Creek mouth Sediment			
Å	2θ (°)	Intensity (counts)	Mineral Phase	Å	2θ (°)	Intensity (counts)	Mineral Phase
14.77	5.99	3121	Chlorite	14.58	6.06	2342	Chlorite
10.19	8.68	17425	illite	10.17	8.69	10667	illite
7.17	12.33	5433	Chlorite	7.17	12.33	4139	Chlorite
5.03	17.62	4976	illite	5.03	17.62	3007	illite
4.3	20.66	2593	quartz	4.3	20.66	4238	quartz
3.61	24.65	1531	kaolinite	3.61	24.66	1018	kaolinite
3.56	24.99	2833	Chlorite	3.56	25.01	2159	Chlorite
3.37	26.44	12828	quartz	3.37	26.44	17999	quartz
3.22	27.68	1688	Chlorite	3.22	27.72	3223	Chlorite
2	45.33	2932	quartz	2	45.36	1870	quartz
1.83	49.94	1171	quartz	1.83	49.95	2209	quartz
1.55	59.76	789	quartz	1.55	59.78	1340	quartz

Appendix B. Colloid Particle Size Characterization

Variability in stream flow due to source discharge presents differing chemical characteristics of water. Warming air temperatures may affect the colloidal composition of suspended solids (e.g. inorganic clays and organic matter) as permafrost degrades and glacial wastage increases (Stolpe et al., 2013). Glacial influenced watersheds have multiple hydrologic pathways that contribute unique suspended loads to streamflow, thus, affecting nutrient availability through geochemical weathering during post-mixing (Richey 1983; Brown et al., 1996; Tranter et al., 2011). The suspended solid contribution in glacial regions has been estimated to account for 76-94% of the sediment load to the Tanana River, Interior Alaska (Wada et al., 2011). Inorganic silt and clay colloids, commonly referred to as glacier flour, are formed from glacier comminution of basal debris and bedrock (Brown et al., 1996; Statham et al., 2008). Colloids 1 nm to1 μm in size are more likely to influence the role in trace metal contaminant transport downstream (Brown et al., 1996; Stolpe et al., 2005; Chanudet and Filella, 2008), and affect dissolved concentrations of bulk stream flow (Brown et al., 1996). Sediment size, chemical characterization and weathering are poorly understood in bulk stream flow and need to be characterized and quantified to predict their role in glacial waters (Brown et al., 1996; Chanudet and Filella, 2008; Stolpe et al., 2013).

Analyses of colloid characterization via field flow fractionation (FFF) techniques are combined with daily stream discharge and chemistry as well as geochemical hydrograph separation techniques to understand the seasonal dependence and export of inorganic nutrients (e.g. silts, clays and iron) and organic matter from Arctic/sub-Arctic terrestrial systems.

Field flow fractionation (FFF) allows for characterization of colloids and separation according to size that are suspended in the water column. A planar column with a flat thin channel is used to focus sample channel flow with an applied external field to the normal flow of FFF. When a cross flow field is applied, particles and solution are forced to an accumulation wall and diffusion is induced. Eventually, these two migration movements reach equilibrium resulting in particle size separation in the sample based on the hydrodynamic diameter of a particle.

An 8mM NaCl solution filtered to less than 0.45 μm with a nylon membrane (Whatman/Schleicher and Schuell (GE Healthcare), USA) was used as a carrier solution. A 1 kDa polyethersulfone (PES) membrane was used to separate colloids coupled with a 412 micrometer spacer (actual width). The injected volume was 0.05 mL of sample. The injection/focusing time was 5 minutes using a cross flow of 3 mL min^{-1}. The cross flow rate was 3 mL min^{-1} for the first

2 minutes followed by a power decay (exp. 0.6) at 3 mL min^{-1} for 55 minutes followed by 10 minutes of 1 mL min^{-1} flow rate. The detector flow was coupled to a UV-detector (PostNova Analytics) operating at dual wavelengths of 254 nm and 280 nm. Three colloid size standards (20 nm, 50 nm, and 100 nm) were analyzed using the same methods (Figure B-1). Given similar operating methods and analytical procedures, elution times of 5-6 minutes can be characterized as humus particles (Benedetti et al., 2002; Piper et al., 2011), 15-30 minutes can be characterized as iron, aluminum and silica particles (Lyvén et al., 2003; Regelink et al., 2013) 70-85 minutes can be characterized as clay particles (illite and kaolinite; Beckett et al., 1997).

Colloidal size characterization of Jarvis Creek samples shows seasonal variation in bulk stream water and glacier terminus water (Figure B-2). Bulk watershed samples were chosen based on seasonal runoff regimes of spring melt, mid-summer and fall. Spring melt sample was defined by peak snow signal in $\delta^{18}O$ analysis (Figure B-3). Mid-summer and fall samples were chosen by date of glacier field sampling campaigns. Normalized UV signal collected during FFF analysis were compared to standards to characterize particle size in water samples. Mid-summer and fall bulk watershed samples are characterized with colloids greater than 50 nm (likely indicative of Fe, Al, Si, and clay minerals), whereas spring samples did not have signals in this size range. May bulk watershed and mid-summer glacier terminus sample were characterized with colloids less than 50 nm in size (likely indicative of humus sized particles). Fall glacier sample showed colloids greater than 50 nm (likely indicative of Fe, Al, Si, and clay size minerals).

FFF analysis shows all samples have particles that are in the same size range as humus (elution time 5-6 minutes, Figure B-2). However, spring stream and summer glacier samples are dominated by particles similar to humus sized particles whereas stream and glacier terminus samples later in the season are dominated by larger particles that are likely indicative of Fe, Al, Si, and clay minerals. The likely humus sized characterization in spring samples compared to samples later in season suggests high amount of overland runoff or near-surface pathways due to spring snowmelt, thus increasing the amount of organic particles in stream runoff. The low signal of humus sized particles in samples later in the season suggests that there is overland runoff from rain events and through flow of soil pore water. Characterization of larger particles (likely Fe, Al, Si, and clays) later in the season suggest high input from waters with a greater degree of geochemical erosion, such as sub-glacial mechanical and chemical erosion. The increase in metal and clay size

particles later in the season agree with the increase in SO_4^{2-}:Cl^- ratios and glacier fractional contribution in June-July of bulk watershed samples (B-3).

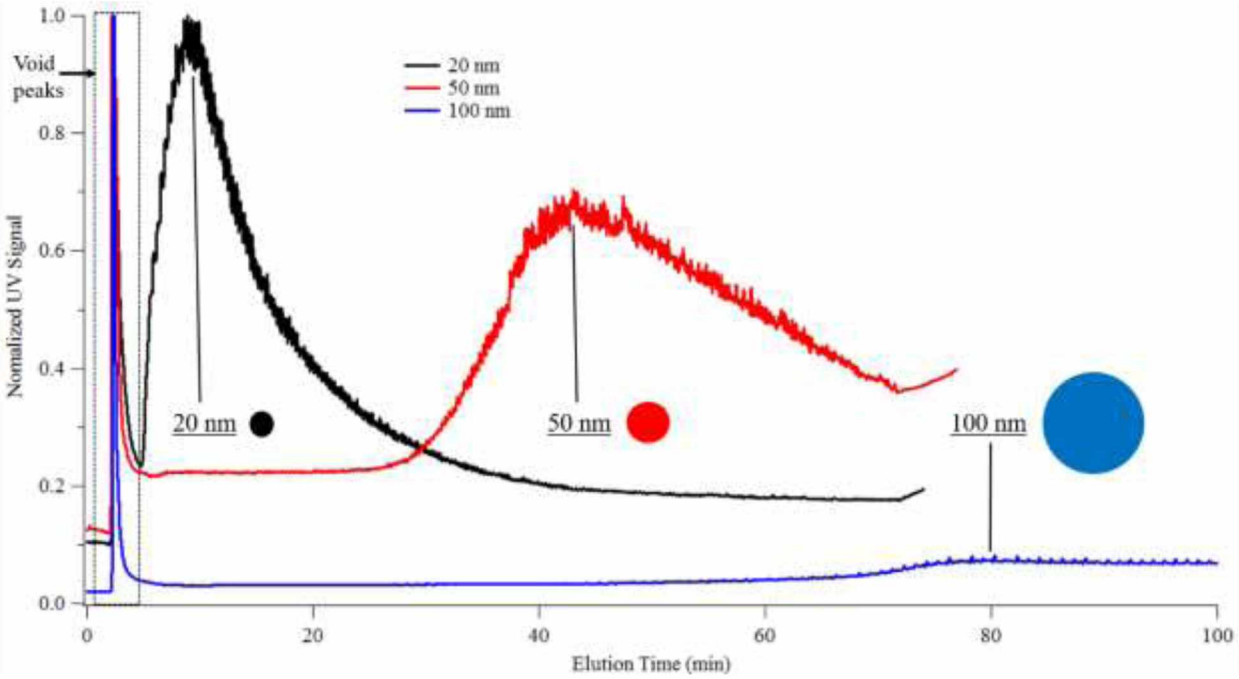

Figure B-1. *Normalized UV signal of 20 nm, 50 nm, and 100 nm standards used for particle size characterization. The first peaks are defined as the void peak.*

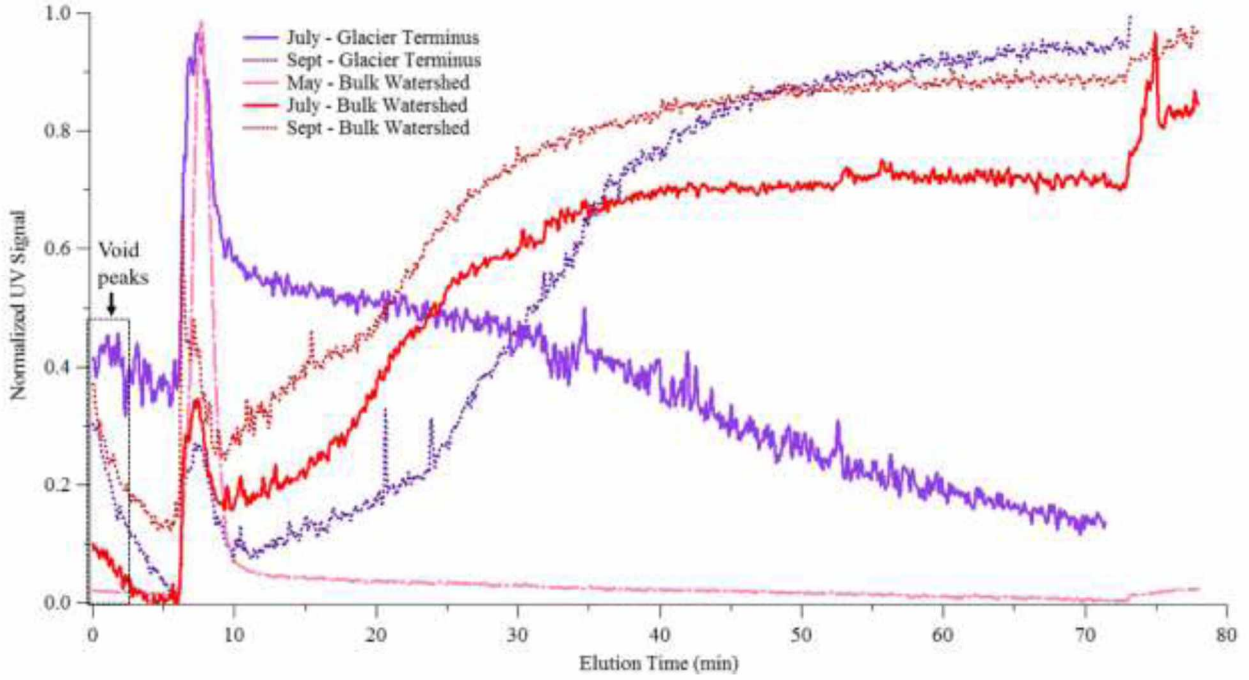

Figure B-2. *Normalized UV signals of Jarvis Creek watershed, 2013. Sample dates are as follow: May 30, 2013; July 18, 2013; September 18, 2013. Particle size characterization is established from standard analysis shown in Figure S.4.a. The first peaks are defined as the void peak.*

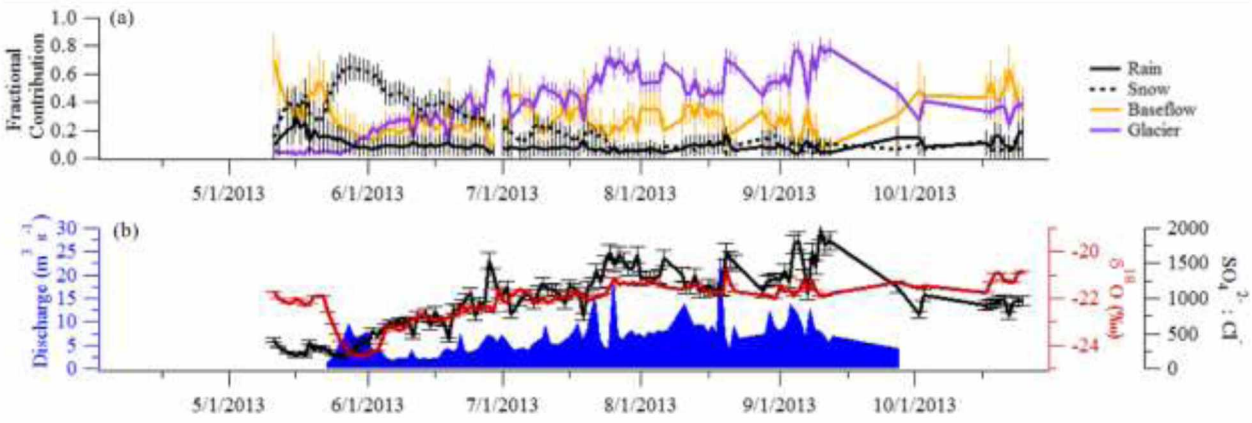

Figure B-3. *2013 Jarvis Creek bulk watershed fractional contributions (a; estimated from geochemical hydrograph separation), stream discharge, $\delta^{18}O$, and SO_4^{2-} : Cl^- ratio (b).*

Appendix C. Local Meteoric Water Line

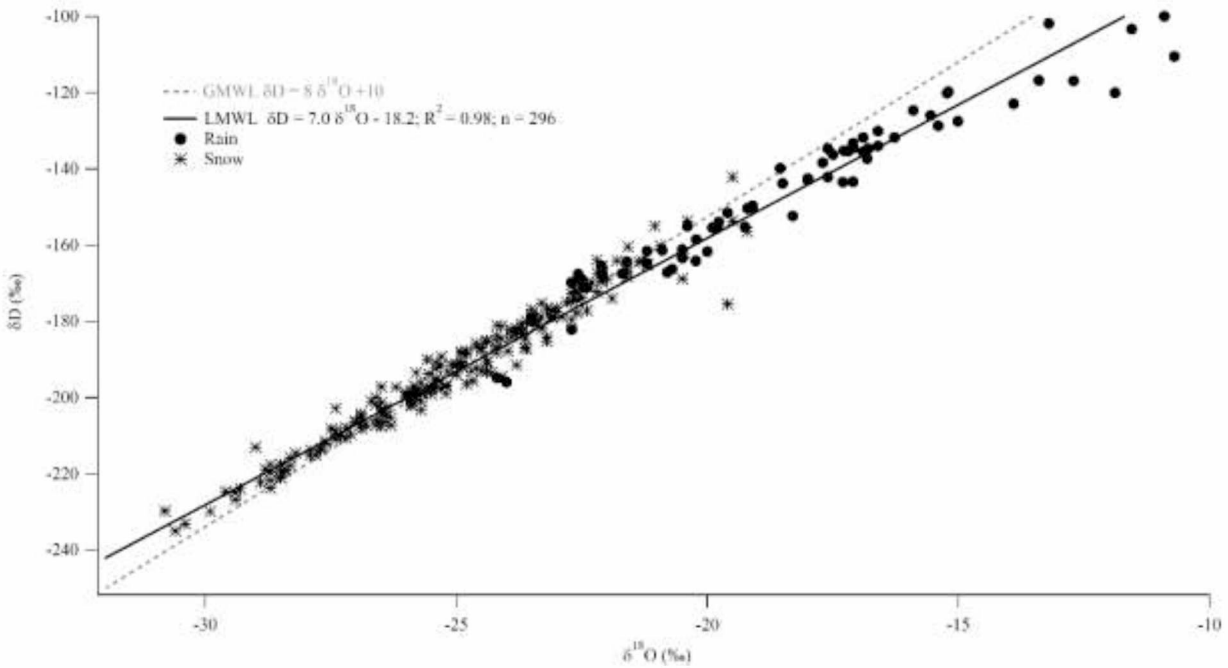

Figure C-1. *Local Meteoric Water Line (LMWL) of Jarvis Creek watershed defined from rain and snow samples collected from 2011-2016 (N = 225 for snow and N = 71 for snow). Black solid line is LMWL ((δD = 7.0 $\delta^{18}O$ – 18.2); grey dotted line is GMWL (δD = 8 $\delta^{18}O$ + 10; Mook, 2000.*

References

Beckett, R., Murphy, D., Tadjiki, S., Chittleborough, D. J., and Giddings, J. C. (1997). Determination of thickness, aspect ratio and size distributions for platey particles using sedimentation field-flow fractionation and electron microscopy. Colloids and Surfaces A: Physicochemical and Engineering Aspects, 120(1-3), 17-26.

Benedetti, M., Ranville, J. F., Ponthieu, M., and Pinheiro, J. P. (2002). Field-flow fractionation characterization and binding properties of particulate and colloidal organic matter from the Rio Amazon and Rio Negro. Organic Geochemistry, 33(3), 269-279.

Brown, G. H., Tranter, M., and Sharp, M. J. (1996). Experimental investigations of the weathering of suspended sediment by alpine glacial meltwater. Hydrological Processes, 10(4), 579-597.

Chanudet, V., and Filella, M. (2008). Size and composition of inorganic colloids in a peri-alpine, glacial flour-rich lake. Geochimica et Cosmochimica Acta, 72(5), 1466-1479.

Lyvén, B., Hassellöv, M., Turner, D. R., Haraldsson, C., and Anderson, K. (2003). Competition between iron-and carbon-based colloidal carriers for trace metals in a freshwater assessed using flow field-flow fractionation coupled to ICPMS. Geochimica et Cosmochimica Acta, 67(20), 3791-3802.

Mook, W.G. ed., (2000). Environmental isotopes in the hydrological cycle: principles and applications; IHP-V. 1. Introduction: theory, methods, review. Unesco.

Regelink, I. C., Weng, L., Koopmans, G. F., and Van Riemsdijk, W. H. (2013). Asymmetric flow field-flow fractionation as a new approach to analyze iron-(hydr) oxide nanoparticles in soil extracts. Geoderma, 202, 134-141.

Richey, J. E. (1983). Interactions of C, N, P, and S in river systems: a biogeochemical model. The Major Biogeochemical Cycles and Their Interactions. Wiley, New York, 365-383.

Statham, P. J., Skidmore, M., and Tranter, M. (2008). Inputs of glacially derived dissolved and colloidal iron to the coastal ocean and implications for primary productivity. Global Biogeochemical Cycles, 22(3).

Stolpe, B., Guo, L., Shiller, A., and Aiken, G. (2013). Abundance, size distributions and trace-element binding of organic and iron-rich nanocolloids in Alaskan rivers, as revealed by field-flow fractionation and ICP-MS. Geochim. Cosmochim. Acta. 105, 221-239.

Stolpe B., Hassellov, M., Andersson, K., and Turner, D. R. (2005). High resolution ICPMS as an on-line detector for flow field-flow fractionation; multi-element determination of colloidal size distributions in a natural water sample. Anal. Chim. Acta 535, 109-121.

Wada, T., Chikita, K. A., Kim, Y., and Kudo, I. (2011). Glacial effects on discharge and sediment load in the subarctic Tanana River Basin, Alaska. Arctic, Antarctic, and Alpine Research, 43(4), 632-648.